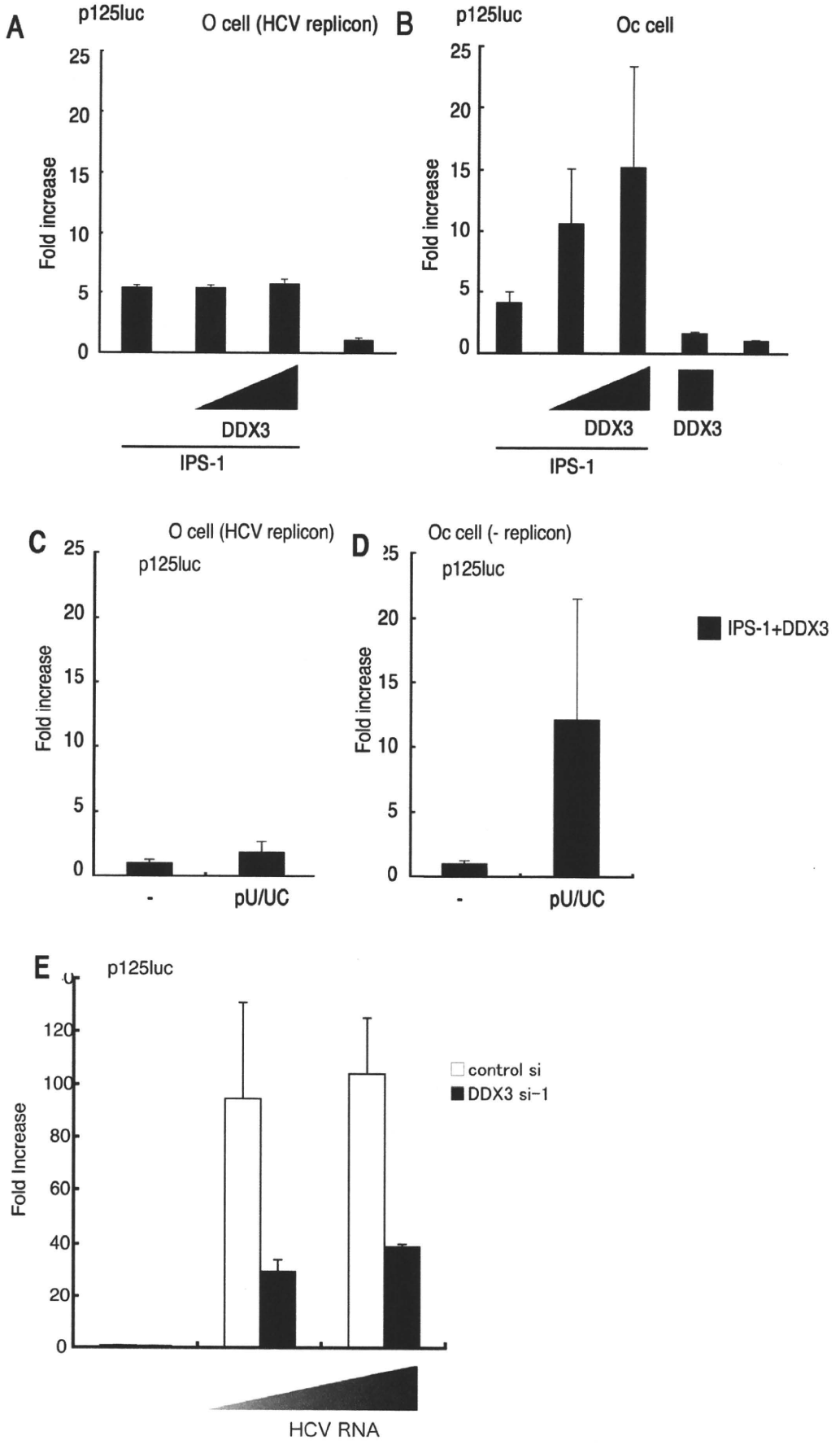
A
p125luc
O cell (HCV replicon)
Fold increase
25
20
15
10
5
0
DDX3
IPS-1
B
p125luc
Oc cell
Fold increase
25
20
15
10
5
0
DDX3
DDX3
IPS-1
C
O cell (HCV replicon)
p125luc
Fold increase
25
20
15
10
5
0
-
pU/UC
D
Oc cell (- replicon)
p125luc
Fold increase
25
20
15
10
5
0
-
pU/UC
IPS-1+DDX3
E
p125luc
Fold Increase
120
100
80
60
40
20
0
control si
DDX3 si-1
HCV RNA

Figure 3. The HCV replicon suppresses IPS-1/DDX3-mediated augmentation of IFN promoter activation. (A,B) O cells with the HCV replicon fail to activate an IFN-β reporter in response to IPS-1/DDX3. O cells contain the full-length HCV replicon, and Oc cells do not [16]. O cells (A) or Oc cells (B) were transfected with IPS-1, DDX3 or p125luc reporter plasmids. At timed intervals (24 hrs), reporter activity was determined as in Fig. 2. (C,D) The HCV replicon suppresses IFN-promoter activation by polyU/UC. O cells and Oc cells expressing IPS-1 and DDX3 were stimulated with polyU/UC. At 48 hrs, reporter activity was determined as in panel A. (E) DDX3 is required for enhanced activation of IFN-beta promoter by O cell HCV 3′UTR. HCV 3′ UTR cDNA was amplified by RT-PCR from RNA extracted from O cells containing full-length HCV replicon. The HCV 3′ UTR RNA was synthesized *in vitro* using T7 RNA polymerase. DDX3 siRNA or control siRNA was transfected into HEK293 cells with the p125luc reporter. After 24 hrs, cells were transfected with HCV RNA, and incubated for 24 hrs. The IFN-beta promoter activation was assessed by luciferase reporter assay. One representative of at least three independent experiments, each performed in triplicate, is shown.
doi:10.1371/journal.pone.0014258.g003

Preparation of HCV polyU/UC RNA

The HCV genotype 1b polyU/UC RNA (from 9421 to 9480, Accession number: EU867431) [23] was synthesized by T7 RNA polymerase *in vitro*. The template dsDNA sequences were; Forward: TAA TAC GAC TCA CTA TAG GGT TCC CTT TTT TTT TTT CTT TTT TTT TTT TTT TTT TTT TTT TTT TTT CTC CTT TTT TTT TC, Reverse: GAA AAA AAA AGG AGA AAA AAA AAA AAA AAA AAA AAA AAA AGA AAA AAA AAA AGG GAA CCC TAT AGT GAG TCG TAT TA. The synthesized RNA was purified by TRIZOL reagent (Invitrogen). cDNA of HCV 3′ UTR region was amplified from total RNA of O cells using primers HCV-F1 and HCV-R1, and then cloned into pGEM-T easy vector. The primer set sequences were HCV-F1: CTC CAG GTG AGA TCA ATA GG and HCV-R1: CGT GAC TAG GGC TAA GAT GG. RNA was synthesized using T7 and SP6 RNA polymerases. Template DNA was digested by DNase I, and RNA was purified using TRIZOL (Invitrogen) according to manufacturer's instructions.

RNAi

Knockdown of DDX3 was carried out using siRNA, DDX3 siRNA-1: 5′-GAU UCG UAG AAU AGU CGA ACA-3′, siRNA-2: 5′-GGA GUG AUU ACG AUG GCA UUG-3′, siRNA-3: 5′-GCC UCA GAU UCG UAG AAU AGU-3′ and control siRNA: 5′-GGG AAG AUC GGG UUA GAC UUC-3′. 20 pmol of each siRNA was transfected into HEK293 cells in 24-well plate with Lipofectamin 2000 according to manufacture's protocol. Knockdown of DDX3 was confirmed 48 hrs after siRNA transfection. Experiments were repeated twice for confirmation of the results.

Reporter assay

HEK293 cells (4×10^4 cells/well) cultured in 24-well plates were transfected with the expression vectors for IPS-1, DDX3 or empty vector together with the reporter plasmid (100 ng/well) and an internal control vector, phRL-TK (Promega) (2.5 ng/well) using FuGENE (Roche) as described previously [23]. The p-125 luc reporter containing the human IFN-beta promoter region (−125 to +19) was provided by Dr. T. Taniguchi (University of Tokyo, Tokyo, Japan). The total amount of DNA (500 ng/well) was kept constant by adding empty vector. After 24 hrs, cells were lysed in lysis buffer (Promega), and the *Firefly* and *Renella* luciferase activities were determined using a dual-luciferase reporter assay kit (Promega). The *Firefly* luciferase activity was normalized by *Renella* luciferase activity and is expressed as the fold stimulation relative to the activity in vector-transfected cells. Experiments were performed three times in duplicate (otherwise indicated in the legends).

PolyI:C or polyU/UC stimulation

PolyI:C was purchased from GE Healthcare company, and solved in milliQ water. For polyI:C treatment, polyI:C was mixed with DEAE-dextran (0.5 mg/ml) (Sigma) in the culture medium, and the cell culture supernatant was replaced with the medium containing polyI:C and DEAE-dextran. Using DEAE-dextran, polyI:C is incorporated into the cytoplasm to activate RIG-I/MDA5.

HCV 3′ UTR poly U/UC region (PU/UC) RNA (0~50 ng/well), which is synthesized *in vitro* by T7 RNA polymerase, transfected into HEK293 cells in 24-well plate by lipofectamin 2000 (Invitrogen) with other plasmids. Cells were allowed to stand for 24~48 hrs and HCV RNA-enhancing activation of IFN-beta promoter was assessed by reporter assay.

Immunoprecipitation (i.p.)

HEK293FT cells were transfected in a 6-well plate with plasmids encoding DDX3, IPS-1, RIG-I or MDA5 as indicated in the figures. 24 hrs after tranfection, the total cell lysate was prepared by lysis buffer (20 mM Tris-HCl [pH 7.5] containing 125 mM NaCl, 1 mM EDTA, 10% Glycerol, 1% NP-40, 30 mM NaF, 5 mM Na_3Vo_4, 20 mM IAA and 2 mM PMSF), and the protein was immunoprecipitated with anti-HA polyclonal (SIGMA) or anti-FLAG M2 monoclonal Ab (SIGMA). The precipitated samples were resolved on SDS-PAGE, blotted onto a nitrocellulose sheet and stained with anti-HA (HA1.1) monoclonal (SIGMA), anti-HA polyclonal or anti-FLAG M2 monoclonal Ab.

Pull-down assay

The pull-down assay was performed according to the method described in Saito T et al. [24]. Briefly, the RNA used for the assay was purchased from JBioS, Co. Ltd (Saitama, Japan). The RNA sequences are (sense strand) AAA CUG AAA GGG AGA AGU GAA AGU G, (antisense strand)CAC UUU CAC UUC UCC CUU UCA GUU U. The biotin is conjugated at U residue at the 3′ end of antisence strand (underlined). Biotinylated double-stranded (ds)RNA were incubated for 1 hr at 25°C with 10 μg of protein from the cytoplasmic fraction of cells that were transfected with Flag-tagged RIG-I and HA-tagged DDX3 expressing vectors. The mixture was transferred into 400 μl of lysis buffer containing 25 μl of streptavidine Sepharose beads, rocked at 4°C for 2 h, collected by centrifugation, washed three times, resuspended in SDS sample buffer.

Proteome analysis of RNA-binding proteins

RNA-binding proteins were identified by affinity chromatography and Mass spectrometry. Briefly, cell lysate was prepared from human HEK293 or Raji cells as will be described elsewhere (Watanabe and Matsumoto, manuscript submitted for publication). The lysate was first applied to polyU-Sepharose and then the pass-through fraction was applied to PolyI:C-Sepharose. The eluted proteins were analyzed on Mass spectrometry using the MASCOT software.

Confocal analysis

HCV replicon-positive (O) or –negative (Oc) cells were plated onto cover glass in a 24-well plate. In the following day, cells were transfected with indicated plasmids using Fugene HD (Roch). The

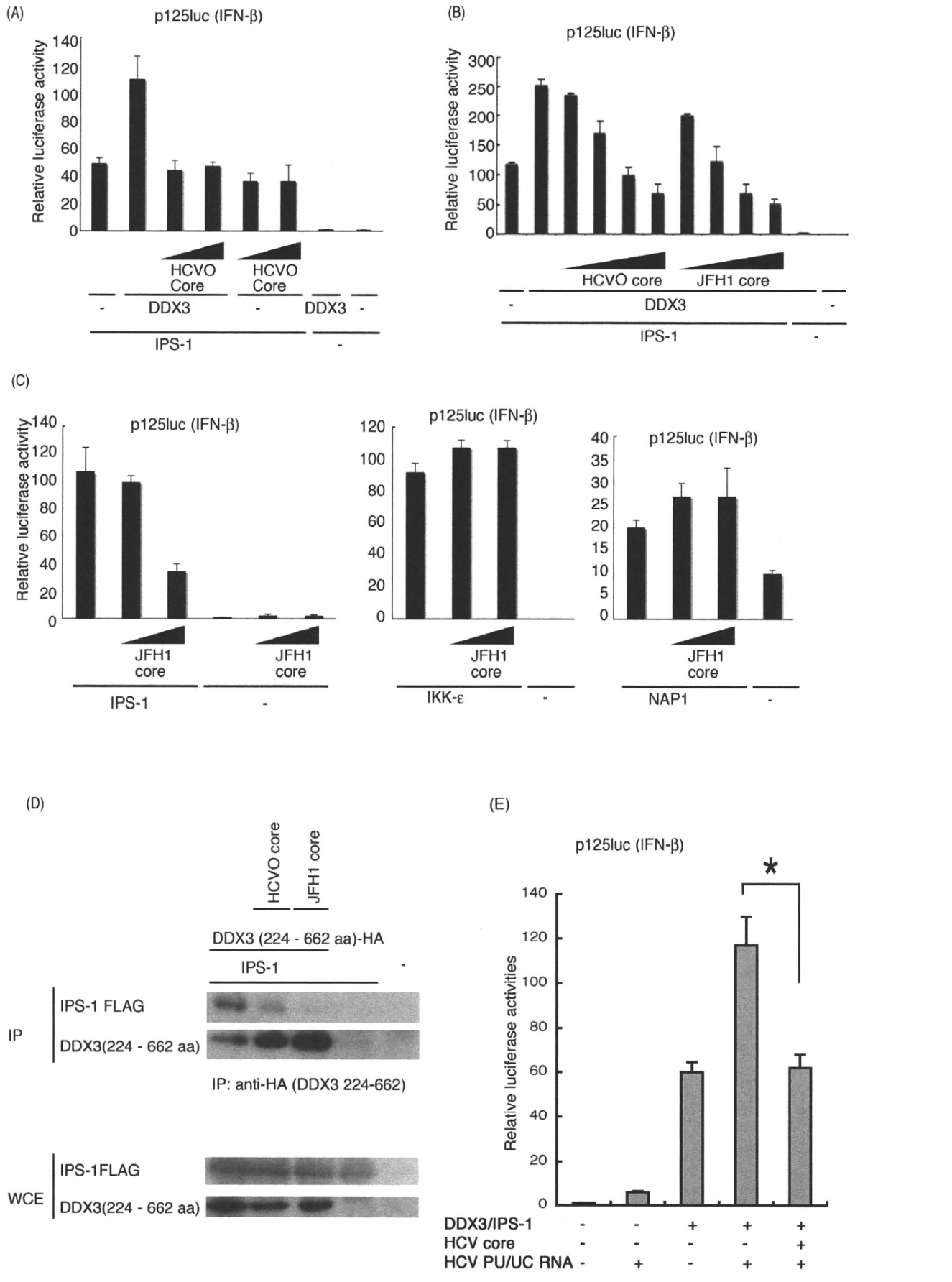
(A)
p125luc (IFN-β)
Relative luciferase activity
140
120
100
80
60
40
20
0
HCVO Core
HCVO Core
-
DDX3
-
DDX3
-
IPS-1
-
(B)
p125luc (IFN-β)
Relative luciferase activity
300
250
200
150
100
50
0
HCVO core
JFH1 core
-
DDX3
-
IPS-1
-
(C)
p125luc (IFN-β)
Relative luciferase activity
140
120
100
80
60
40
20
0
JFH1 core
JFH1 core
IPS-1
-
p125luc (IFN-β)
120
100
80
60
40
20
0
JFH1 core
IKK-ε
-
p125luc (IFN-β)
40
35
30
25
20
15
10
5
0
JFH1 core
NAP1
-
(D)
HCVO core
JFH1 core
DDX3 (224 - 662 aa)-HA
IPS-1
-
IP
IPS-1 FLAG
DDX3(224 - 662 aa)
IP: anti-HA (DDX3 224-662)
WCE
IPS-1FLAG
DDX3(224 - 662 aa)
(E)
p125luc (IFN-β)
*
Relative luciferase activities
140
120
100
80
60
40
20
0
DDX3/IPS-1 - - + + +
HCV core - - - - +
HCV PU/UC RNA - + - + +

Figure 4. HCV core protein inhibits DDX3 promotion of IPS-1-mediated IFN-beta induction. (A) Expression plasmids for IPS-1 (100 ng), DDX3 (200 ng) and/or HCVO core (50 or 100 ng) were transfected into HEK293 cells in 24-well plates with reporter plasmids, and reporter activity was examined. (B) Expression plasmids for IPS-1 (100 ng), DDX3 (100 ng), and/or HCVO or JFH1 core (10, 25, 50 or 100 ng) were transfected into HEK293 cells, and reporter gene expression was analyzed. (C) IPS-1-, IKKepsilon- or NAP1-expressing plasmids were transfected into HEK293 cells with HCV JFH1 core-expressing plasmids (25 or 100 ng), for reporter gene analysis. (D) Plasmids for expression of FLAG-tagged IPS-1 (400 ng), HA-tagged DDX3 partial fragment (400 ng) and HCVO or JFH1 core (400 ng) were transfected into HEK293FT cells. 24 hrs later cells were lyzed and the lysate was incubated with anti-HA Ab for immunoprecipitation. The DDX3 (224-662)-bound IPS-1 was blotted onto a sheet and probed with anti-Flag Ab. Whole cell lysate was also stained with anti-tag Abs. (E) IPS-1 (100 ng), DDX3 (100 ng), JFH1 core (50 ng) and/or p125 luc reporter (100 ng) plasmids were transfected with HEK293 cells, with HCV 3′UTR poly-U/UC (PU/UC) RNA (25 ng), synthesized *in vitro*. Cell lysates were prepared after 24 hrs, and luciferase activities measured. One representative of at least three independent experiments is shown except for panel D, which is a representative of two sets of the experiments.
doi:10.1371/journal.pone.0014258.g004

amount of DNA was kept constant by adding empty vector. After 24 hrs, cells were fixed with 3% of paraformaldehyde in PBS for 30 minutes, and then permeabilized with PBS containing 0.2% of Triton X-100 for 15 min. Permeabilized cells were blocked with PBS containing 1% BSA, and were labeled with anti-Flag M2 mAb (Sigma) or anti-HA pAb (Sigma) in 1% BSA/PBS for 1 hr at room temperature [25]. In some cases, endogenous proteins were directly stained with anti-core (C7-50) mAb (Affinity BioReagents, Inc) or anti-DDX3 pAbs (Abcam, Cambridge MA). The cells were then washed with 1% BSA/PBS and treated for 30 min at room temperature with Alexa-conjugated antibodies (Molecular Probes). Thereafter, micro-cover glass was mounted onto slide glass using PBS containing 2.3% DABCO and 50% of glycerol. The stained cells were visualized at ×60 magnification under a FLUOVIEW (Olympus, Tokyo, Japan).

Results

DDX3 binds RNA species

We have performed proteome analyses of RNA-binding fractions in human dendritic cell lysate eluted from polyU and polyI:C Sepharose. 127 cytoplasmic proteins were reproducibly identified as polyI:C-binding proteins (Watanabe and Matsumoto, unpublished data). Four of them are DEAD/H box helicases. In this setting, we found DDX3 is a RNA-binding protein (Fig. 1A). DDX3 in cell lysate bound both polyU and polyI:C, while the control PKR bound only to polyI:C.

Using biotinylayed dsRNA, RNA-binding properties of DDX3 and RIG-I were tested by pull-down assay. DDX3 or RIG-I protein was co-precipitated with dsRNA in HEK293 cells expressing either alone of DDX3 or RIG-I (Fig. 1B). Strikingly, higher amounts of DDX3 and RIG-I were precipitated with dsRNA in cells expressing both proteins (Fig. 1B). This, taken together with previous results [11,14,16], indicates that DDX3 assembles in some RNA, RIG-I, IPS-1 and HCV core protein in its C-terminal domain (Fig. S1).

PolyU/UC but not replicon enhances IFN-β induction via IPS-1/DDX3

A polyU/UC sequence is present in the 3′-region of the HCV genome, and serves as a ligand for RIG-I in IPS-1 pathway activation [23]. We produced the polyU/UC RNA and tested its IFN-beta-inducing activity in the presence or absence of DDX3 and IPS-1 (Fig. 2A). HCV polyU/UC promoted IPS-1-mediated IFN-beta induction, and this was further enhanced by forced expression of DDX3/IPS-1 (Fig. 2A). Similar results were obtained with wild-type mouse embryonic fibroblasts (MEF) (Fig. 2B). We also investigated whether DDX3 enhanced IPS-1-mediated IFN-β promoter activation in a RIG-I −/− MEF background (Fig. 2B). In IPS-1/DDX3-expressing MEF cells, polyU/UC IFN-induction was almost totally abrogated by the lack of RIG-I, suggesting that the trace RIG-I protein in the IPS-1 complex is required for DDX3 enhancement of the polyU/UC-mediated IFN response.

DDX3 mRNA (Fig. 2C) and protein [11] were depleted in HEK293 cells by gene silencing with si-1 siRNA, so this was used for DDX3 loss-of-function analysis. Control or DDX3-silinced cells were transfected with increasing amounts of polyU/UC and IFN-beta promoter activation was determined by luciferase assay. DDX3 loss-of-function resulted in a decrease of promoter activation by intrinsic polyU/UC (Fig. 2D). The result was confirmed with cells over-expressing RIG-I and exogenous polyI:C stimulation. HEK293 cells were transfected with a plasmid for the expression of RIG-I and stimulated with polyI:C, an activator of the IPS-1 pathway (Fig. S2A). IFN-beta reporter activation was suppressed in si-1-treated cells that expressed RIG-I, since polyI:C lots often contain short size duplexes that can activate RIG-I [26]. In addition, DDX3 augmented the IFN-beta response in cells expressing MDA5/IPS-1 (Fig. S2B). Thus, DDX3 was also crucial for IPS-1-mediated IFN-beta promoter activation.

We next determined whether the HCV replicon triggers IPS-1/DDX3 IFN promoter activation, using human hepatocyte lines with the HCV replicon (O cells) or without it (Oc cells). In O cells with the HCV replicon, IPS-1/DDX3 expression showed minimal enhancement of IFN-beta promoter activation (Fig. 3A), while in control Oc cells with no replicon, DDX3 facilitated IFN-beta promoter activation (Fig. 3B). Similarily, an augmented IFN promoter response to polyU/UC was observed in control Oc cells, but not in O cells (Figs. 3C and 3D). HCV RNA was prepared from O cells, and its ability to activate the IFN-beta reporter was tested in HEK293 cells (Fig. 3E). The HCV RNA of O cells had a high potency to induce reporter activation, and this activity was largely abrogated by si-1 siRNA treatment. Therefore, DDX3 augments IPS-1-mediated IFN-beta promoter activation in hepatocyte O cells, and HCV RNA, presumably the 3′UTR, participates in this induction. However, no IFN-beta reporter activation was detected in O cells which harbor HCV replicon. Therefore, an unidentified viral factor appeared to participate in suppressing virus RNA-mediated IFN-beta induction, which occurred in O cells overexpressing DDX3/IPS-1.

HCV core protein inhibits IPS-1 signaling through DDX3

What HCV proteins participate in IFN-beta induction was tested in a pilot study using protein expression analysis. We found that expression of HCV core protein as well as NS3/4A led to suppression of IFN-beta reporter activity in Oc cells (data not shown). The HCV core protein physically binds DDX3 [14,16], and co-localizes with DDX3 in the cytoplasm of HeLa cells transfected with HCV core protein [14]. Furthermore, we showed that DDX3 binds IPS-1, which resides on the mitochondrial outer membrane, and assembles into RNA-sensing receptors. Since some populations of the HCV core protein localize on the mitochondrial outer membrane [27], we tested if HCV core

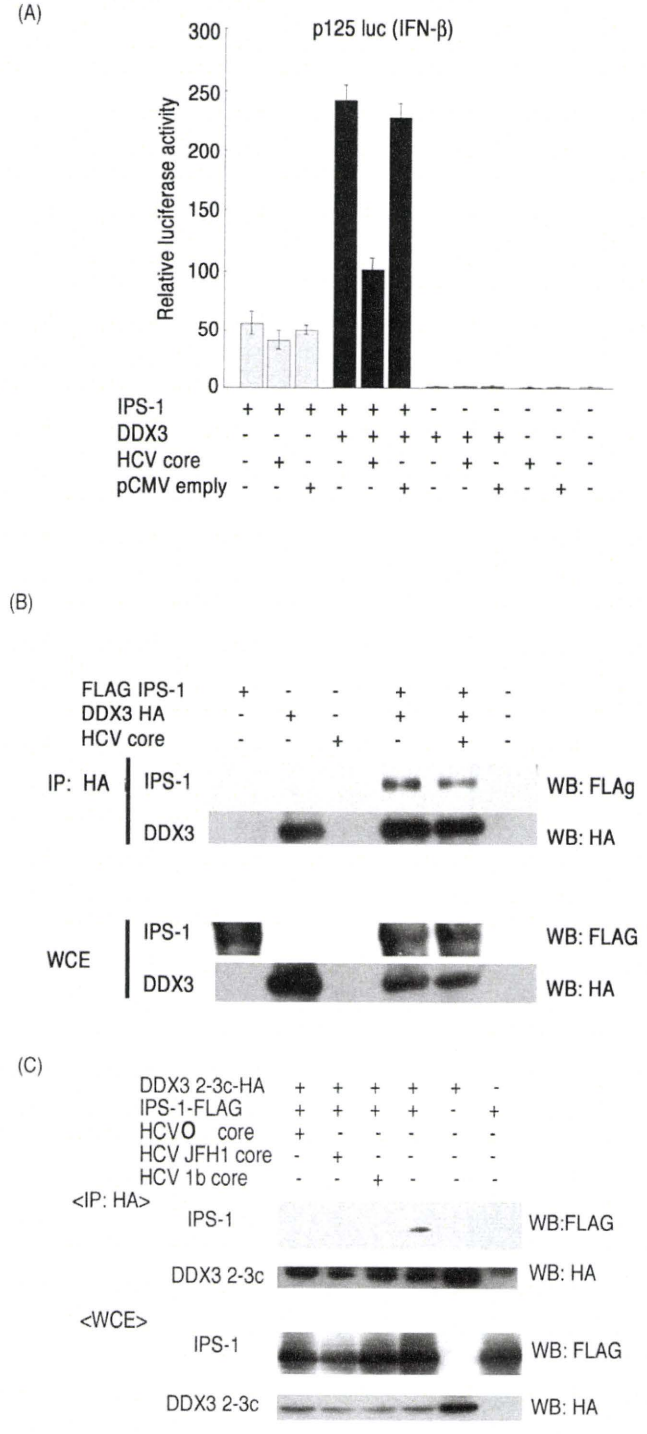

Figure 5. Properties of a 1b-type core protein in the IPS-1 pathway. (A) A core protein derived from an HCV patient suppressed DDX3-mediated activation of IPS-1 signaling. The 1b-type core protein was cloned into the pCMV vector from a patient with hepatitis C. IPS-1 (100 ng), DDX3 (100 ng) and HCV core (100 ng) expression vectors were transfected into HEK293 cells with a reporter plasmid (p125luc), for analysis as in Figure 4. (B) The core protein reduced interaction between full-length DDX3 and IPS-1. The plasmids encoding core protein (400 ng), DDX3-HA (400 ng) and FLAG-IPS-1 (400 ng) were transfected into HEK293FT cells. After 24 hrs, cell lysates were prepared and immunoprecipitation was carried out using anti-HA (DDX3-HA). (C) The core protein blocked interaction between the C-terminal fragment of DDX3 and IPS-1. The C-terminal region of DDX3 (199–662 aa) called DDX3 2-3c, IPS-1, HCV (O) and JFH1 or 1b core expression plasmids were transfected into HEK293FT cells. After 24 hrs, cell lysates were prepared and immunoprecipitation was carried out with anti-HA (DDX3 2–3c). Immunoprecipitates were analyzed by SDS-PAGE and Western blotting with anti-HA or FLAG antibodies. The results are representative of two independent experiments.
doi:10.1371/journal.pone.0014258.g005

protein affects IPS-1 signaling by binding to DDX3. The cDNAs for HCV core proteins, genotype 1b (HCVO) and 2a (JFH1) [16], were co-transfected into HEK293 together with IPS-1, DDX3, and reporter plasmids, and core protein interference with IPS-1/DDX3-mediated IFN-beta promoter activation was examined. We found that the core proteins of HCVO and JFH1 suppressed IPS-1/DDX3-augmented IFN-beta-induction in a dose-dependent manner (Fig. 4A and 4B). Without DDX3 transfection, core protein had no effect on IPS-1-mediated IFN-beta promoter activation (Fig. 4A). JFH1 core slightly more efficiently inhibited IPS-1/DDX3-augmented IFN-beta-induction than HCVO core (Fig. 4B).

Although some endogenous DDX3 was present in the cytoplasm without DDX3 transfection, only IPS-1 transfection permitted minimal induction of IFN-beta. It is notable that high doses of the HCV JFH1 core protein was needed to inhibit the IPS-1-mediated IFN-beta-induction signal (Fig. 4C, left panel). Since the imaging profile of DDX3 is not always monotonous in human cells, its distribution may be biased in the cytoplasm, which may reason that only a high dose of HCV core involves preoccupied DDX3 protein to inhibit the IPS-1 pathway. This is consistent with earlier reports on an NS3-independent mechanism to block IFN induction using HCV-infected Huh 7 cells [28].

IPS-1 transduces a RNA replication signal to result in IFN-beta output using downstream proteins, such as NAP1 and IKKeysilon. If the HCV core protein interferes with IPS-1 function through DDX3, the core should not inhibit over-expressed downstream molecules. As predicted, HCV core protein did not suppress the IKKepsilon- or NAP1-mediated IFN-beta-inducing signal (Fig. 4C, center and right panels). Hence, the core protein blocks the action of endogenous DDX3 and overexpressed IPS-1 to facilitate minimal IFN-beta promoter activation, and this IFN-beta blocking function of core does not target IKKepsilon or NAP1 (Fig. 4C). An upstream molecule of IKKepsilon and NAP1 is predicted to be the target of the HCV core protein, which is in line with the fact that the HCV core protein interacts with DDX3 [14,16].

To further confirm this model, we examined whether the HCV core protein inhibits the physical interaction between IPS-1 and DDX3. Full length IPS-1 and the C-terminal fragment of DDX3, which binds to the IPS-1 CARD-like region, were transfected into HEK293 cells, with or without the HCV core protein, and the DDX3 fragment was immunoprecipitated. Expression of HCV core proteins strongly inhibited interaction between the DDX3 C-terminal fragment and IPS-1 (Fig. 4D). JFH1 core appeared to show greater inhibition to DDX3-IPS-1 interaction than HCVO. We then examined this IFN-beta blocking function of JFH1 core in a similar cell condition plus polyU/UC. DDX3/IPS-1-enhanced p125luc reporter activity in cells stimulated with polyU/UC (Fig. 4E) was decreased in cells expressing HCV core. The results suggest that the role of the core in HCV-infected cells is to remove DDX3 from IPS-1, and facilitate its interaction with HCV replication complex (Fig. S1).

PolyU/UC HCV RNA activates the IFN-beta promoter (Fig. 2A), and this activity was inhibited by expression of the HCV core protein (Fig. 4E). PolyI:C/RIG-I-mediated IFN-β promoter activation was similarly suppressed by the core protein

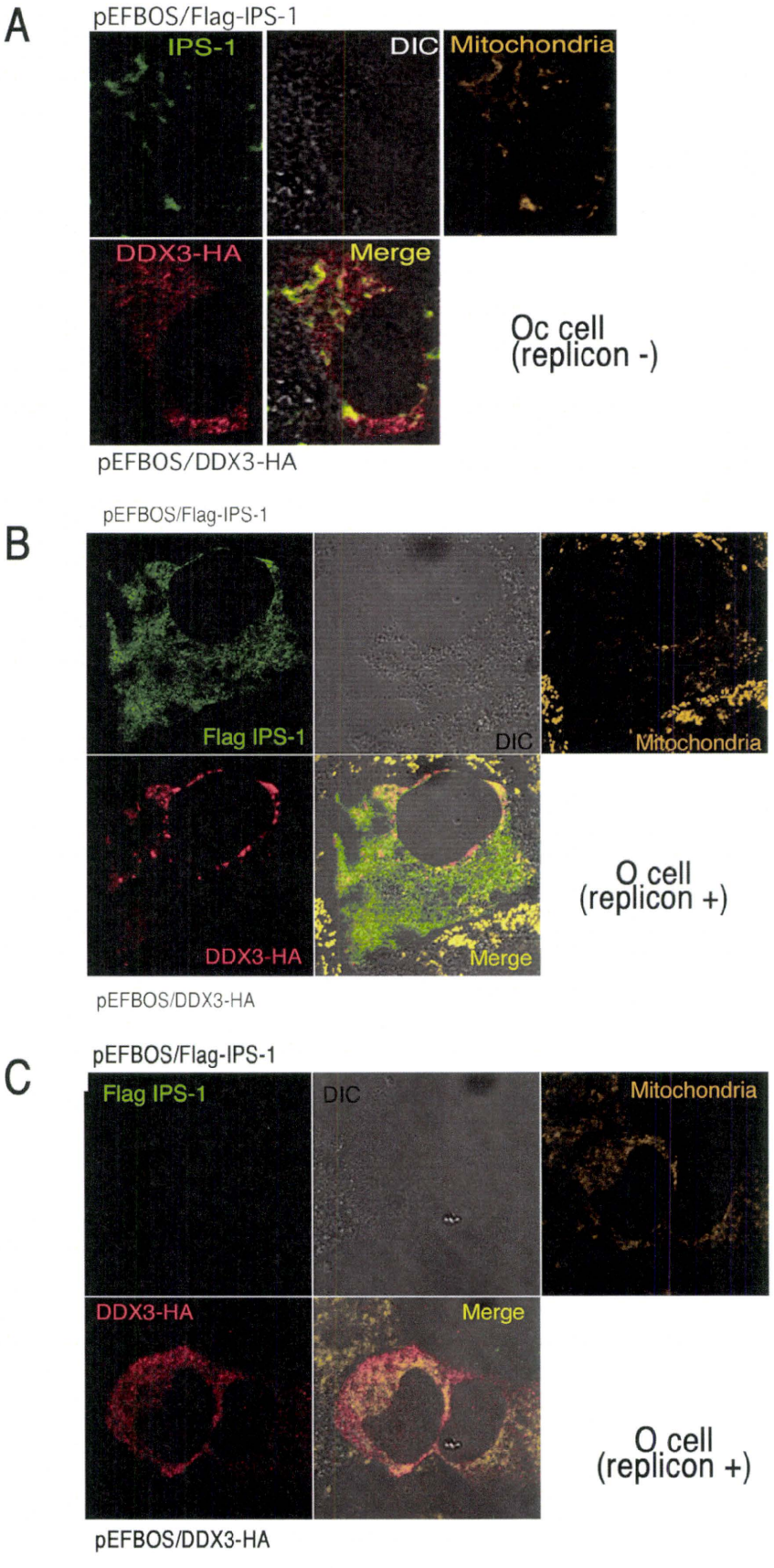
A
pEFBOS/Flag-IPS-1
IPS-1
DIC
Mitochondria
DDX3-HA
Merge
Oc cell
(replicon -)
pEFBOS/DDX3-HA
B
pEFBOS/Flag-IPS-1
Flag IPS-1
DIC
Mitochondria
DDX3-HA
Merge
O cell
(replicon +)
pEFBOS/DDX3-HA
C
pEFBOS/Flag-IPS-1
Flag IPS-1
DIC
Mitochondria
DDX3-HA
Merge
O cell
(replicon +)
pEFBOS/DDX3-HA

Figure 6. Distribution of DDX3 and IPS-1. (A) DDX3 colocalizes with IPS-1 on the mitochondria in Oc cells. HA-tagged DDX3 and FLAG-tagged IPS-1 were co-transfected into Oc cells. After 24 hrs, cells were fixed with formaldehyde and stained with anti-HA polyclonal and FLAG monoclonal Abs. Alexa488 (DDX3-HA) or Alexa633 antibody was used for second antibody. Mitochondria were stained with Mitotracker Red. Similar IPS-1-DDX3 merging profiles were observed in Huh7.5.1 cells (Fig. S3). (B,C) O cells with the HCV replicon poorly formed the DDX3-IPS-1 complex. Plasmids carrying IPS-1 (100 ng) or DDX3 (150 or 300 ng) were transfected into O (HCV replicon +) as in Oc cells (no replicon, panel A). After 24 hrs, localization of IPS-1 and DDX3 was examined by confocal microscopy. Two representatives which differ from the conventional profile (as in panel A) are shown. Similar sets of experiments were performed four times to confirm the results.
doi:10.1371/journal.pone.0014258.g006

(Fig. S2A). MDA5-dependent IFN-beta promoter activation was also suppressed by the core expression (Fig. S2B). The inhibitory effect of the core protein on DDX3-IPS-1 interaction was further confirmed using an 1b core isoform isolated from a patient. This HCV core protein also reduced interaction as well as IPS-1-mediated IFN-beta promoter activation (Fig. 5A). The blocking effect was relatively weak in cells expressing IPS-1 and full-length DDX3 (Fig. 5B). We presume that this is because there are multiple binding sites for IPS-1 in the DDX3 whole molecule [11]. For binding assay, we used DDX3 2-3c (across a.a. 199~662, longer than 224~662) instead of the whole DDX3. In fact, DDX3(199-662)-IPS-1 interaction was blocked by the additional expression of core protein (HCVO, JFH1 or 1b core) in Fig. 5C. Ultimately, HCV core protein suppresses IPS-1 signaling by blocking the interaction between the C-terminal region of DDX3 and the CARD-like region of IPS-1, and this inhibition apparently causes the disruption of the active RIG-I/DDX3/IPS-1 complex that efficiently induces IFN-beta production signaling.

Localization of DDX3 and HCV core protein in O cells

We attempted to confirm this finding by tag-expressed proteins and imaging analysis. In Huh7.5 cells IPS-1 colocalized with DDX3 around the mitochondria (Fig. S3), and so did in the hepatocyte lines Oc cells with no HCV replicon (Fig. 6A). In Oc and Huh7.5.1 cells with no HCV replicon, abnormal distribution of IPS-1 was barely observed (Fig. 6A, Fig. S3). In O cells expressing DDX3 and IPS-1, by contrast, two distinct profiles of IPS-1 were observed in addition to the Fig. 6A pattern of IPS-1: diminution or spreading of the IPS-1 protein over mitochondria (Fig. 6B,C). IPS-1 may be degraded by NS3/4A in some replicon-expressing O cells as reported previously [5,28]. We counted number of cells having the pattern represented by Fig. 6 panel B and those similar to Fig. 6 panel C, and in most cases the latter patterns were predominant.

What happens in the O cells with replicon when the core protein is expressed was next tested. Using O and Oc cells, we tested the localization of the core protein and DDX3 in comparison with IFN-inducing properties (Fig. 3). In O cells with full-length HCV replicon, DDX3 was localized proximal to the lipid droplets (LD) (Fig. 7A top panel) around which HCV particles assembled [29]. HCV core protein and DDX3 were partly colocalized in the HCV replicon-expressing cells (Fig. 7A center panel). The results were confirmed with HCV replicon-expressing O cells where endogenous core and DDX3 were stained (Fig. 7B upper panel). Partial merging between core and DDX3 was reproduced in this case, too. In contrast, sO cells, which possess a subgenomic replicon lacking the cording region of the core protein, showed no merging profile of DDX3 and LD (Fig. 7A bottom panel). Likewise, Oc cells barely formed assembly consisting of LD (where the core assembles) and overexpressed DDX3 (Fig. 7A bottom panel) or endogenous DDX3 (Fig. 7B lower panel). O cells expressing DDX3 tended to form large spots compared to Oc cells (with no replicon) and sO cells (core-less replicon) with DDX3.

Overexpressed DDX3 allowed the Oc cells to induce IPS-1-mediated IFN-beta promoter activation (Fig. 3B), while this failed to happen in O cells having HCV replicon (Fig. 3A). Ultimately, overexpressed IPS-1 did not facilitate efficient merging with DDX3 in O cells with replicon (Fig. 6B,C) compared to Oc cells or Huh7.5 cells with no replicon (Fig. 6A, Fig. S3). The results on the functional and immnoprecipitation analyses, together with the imaging profiles, infer that the IPS-1-enhancing function of DDX3 should be blocked by both NS3/4A-mediated IPS-1 degradation and the HCV core which translocates DDX3 from the IPS-1 complex to the proximity of LD in HCV replicon-expressing cells.

Discussion

We investigated the effect of the HCV core protein on the cytosolic DDX3 that forms a complex with IPS-1 to enhance the RIG-I-mediated RNA-sensing pathway. We demonstrated that the core protein removes DDX3 from the IFN-β-inducing complex, leading to suppression of IFN-β induction. DDX3 is functionally complex, since its protective role against viruses may be modulated by the synthesis of viral proteins. DDX3 acts on multiple steps in the IFN-inducing pathway [30]. In addition, DDX3 interacts with the HCV core protein in HCV-infected cells and promotes viral replication [16]. This alternative function is accelerated by the HCV core protein, resulting in augmented HCV propagation [14,16]. More recently, Patal et al., reported that interaction of DDX3 with core protein is not critical for the support of viral replication by DDX3, although DDX3 and core protein colocalize with lipid droplet [15]. If this is the case, what function is revealed by the interaction between DDX3 and HCV core protein remain unsettled. At least, HCV replication is not blocked by this molecular interaction [15].

It remains unclear in Fig. 4C why higher doses of JFH1 core protein are required to inhibit enhancement of IPS-1 signaling by endogenous DDX3 than by exogenously overexpressed DDX3. One possibility is that endogenous DDX3 is preoccupied in a molecular complex other than the IPS-1 pathway since DDX3 is involved in almost every step of RNA metabolism and its localization affects its functional profile [18,30].

Together with these findings, the results presented here suggest that the HCV core inactivates IPS-1 in a mode different from NS3/4A [5,31]. The core protein may switch DDX3 from an antiviral mode to an HCV propagation mode. The core protein localizes to the N-terminus of the HCV translation product, and is generated in infected cells before NS3/4A proteolytically liberates non-structural proteins and inactivates IPS-1. Our results on how the HCV core protein interferes with the interaction between DDX3 and IPS-1 add several possibilities to notions about the HCV function on the IFN-beta-inducing pathway [18].

DDX3 appears to be a prime target for viral manipulation, since at least three different viruses, including HCV [14], Hepatitis B virus [32], and poxviruses [8], encode proteins that interact with DDX3 and modulate its function. These viruses seem to co-opt DDX3, and also require it for replication. The viruses are all oncogenic, and may confer oncogenic properties to DDX3.

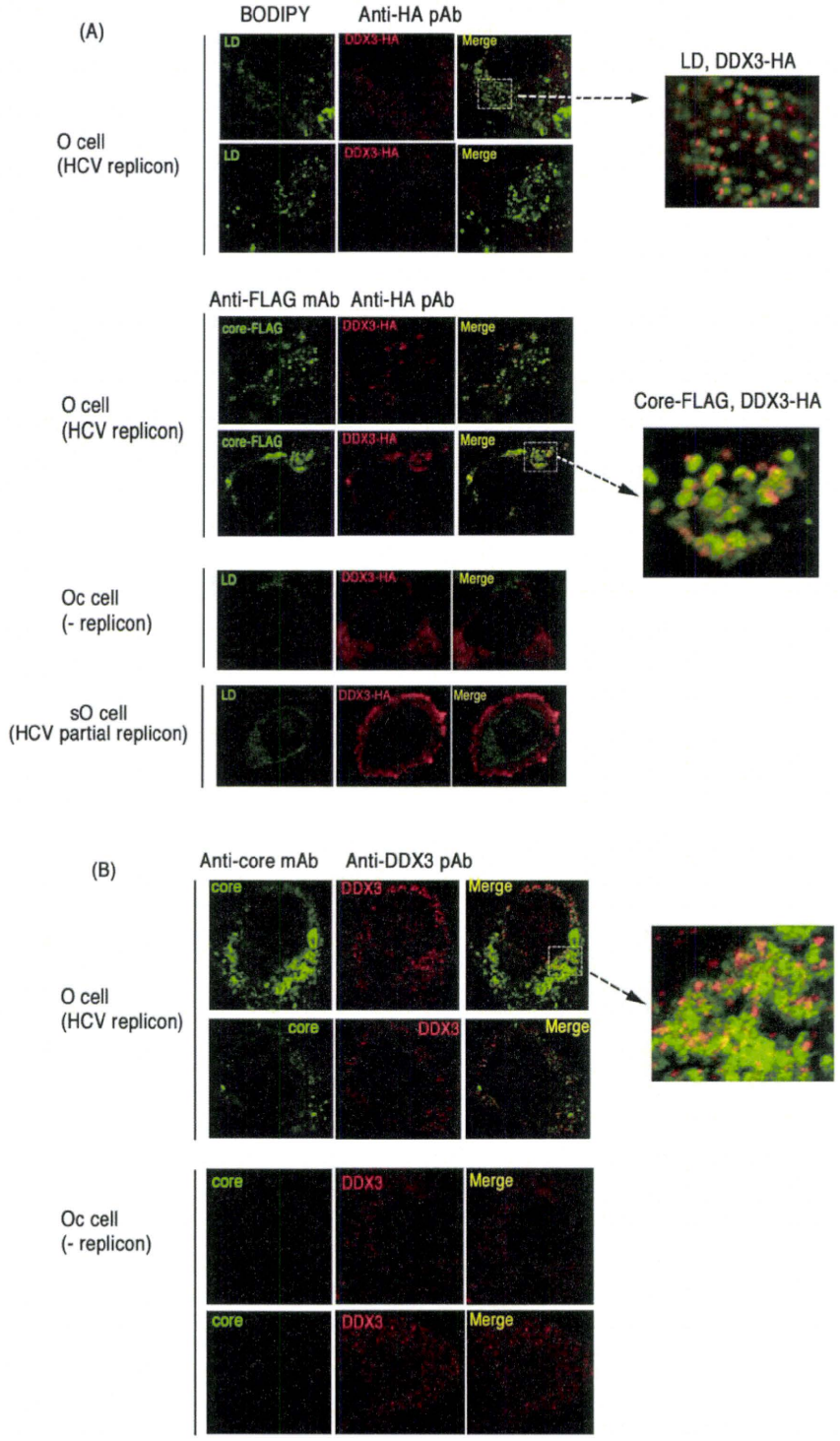

Figure 7. Partial association of endogenous and overexpressed DDX3 with HCV core protein in hepatocyte lines. (A) O cells with the HCV replicon form DDX3-containing speckles in the cytoplasm. O cells contain full-length HCV replicon, and Oc cells do not [16]. O cells were transfected with a plasmid expressing HA-tagged DDX3 (top panel). In other experiments, O cells were transfected with plasmids expressing HA-tagged DDX3 and FLAG-tagged HCV core protein (center panel). After 24 hrs, cells were stained with anti-HA or FLAG antibodies. Proteins were visualized with Alexa488 or 564 second antibodies and the LD was stained with BODIPY493/503. In the bottom panel, Oc cells (no replicon) and sO cells with the core-less subgenomic replicon [16] were transfected with a plasmid expressing HA-tagged DDX3. After 24 hrs, cells were stained with anti-HA antibodies. LD was stained with BODIPY493/503. (B) Endogenous DDX3-HCV core association in O cells. O or Oc cells were cultured to amplify the HCV replicon. Cells were stained with anti-core mAb and anti-DDX3pAb and secondary antibodies. Similar sets of experiments were performed three times to confirm the results.
doi:10.1371/journal.pone.0014258.g007

DDX3 is also involved in human immunodeficiency virus RNA translocation [33]. The DDX3 gene is conserved among eukaryotes, and includes the budding yeast homolog, Ded1 [34]. The Ded1 helicase is essential for initiation of host mRNA translation, and human DDX3 complements the lethality of Ded1 null yeast [14,35]. Another function of DDX3 is to bind viral RNA to modulate RNA replication and translocation. Constitutive expression of the HCV core or other DDX3-binding proteins may impede IFN induction and promote cell cycle progression. These reports are consistent with the implication of DDX3 in various steps of RNA metabolism in cells that contain both host and viral RNAs.

A continuing question is the physiological role of the molecular complex of DDX3 and IPS-1 during replication of HCV in hepatocytes. HCV proteins generated in host hepatocytes usually induce an HCV-permissive state in patients, for example in the IFN-inducing pathways. NS3/4A protease induces rapid degradation of IPS-1 [5,31] and TICAM-1/TRIF [36]. NS5A interferes with the MyD88 function [37]. Viral replication ultimately blocks the STAT1-mediated IFN-amplification pathway [38]. PKR may be an additional factor by which HCV controls type I IFN production [39]. Our results add to our knowledge of the mechanism of how HCV circumvents IFN induction in host cells: HCV core protein suppresses the initial step of IFN-beta induction by interfering with DDX3-IPS-1 association. Indeed, the core protein functions as the earliest IFN suppressor, since it is generated first in HCV-infected cells, and rapidly couples with DDX3 to retract it from the IPS-1 complex, resulting in localization of DDX3 near the LD (Fig. 7). It is HCV that hijacks this protein for establishing infection. Although gene disruption of DDX3 makes mice lethal, this issue will be further tested using IPS-1 $-/-$ hepatocytes expressing human CD81 and occludin [40], in which HCV replication would proceed.

DDX3 primarily is an accelerating factor for antiviral response through IPS-1-binding. Many host proteins other than DDX3 may positively regulate HCV replication in hepatocytes in association with the IPS-1 pathway. In this context, we know LGP2 [41] and STING [42] act as positive regulators in virus infection. Peroxisomes serve as signaling platforms for recruiting IPS-1 with a different signalosome than mitochondria [43]. It appears rational that HCV harbors strategies to circumvent these positive regulators in the relevant steps of the IFN-inducing pathway.

Imaging studies suggest that the complex of IPS-1 involving the membrane of mitochondrial/peroxisomes differ from that free from the membrane. Although IPS-1 is liberated from the membrane by NS3/4A having largely intact cytosolic domain, it loses the IFN-inducing function [5,31]. Our results could offer the possibility that the clipped-out form of IPS-1 immediately fails to form the conventional complex for IRF-3 activation any more [44] or is easily degraded further to be inactive (Fig. 6C). Indeed, there are a number of mitochondria-specific molecules which assemble with IPS-1 [45]. Formation of the molecular complex on the mitochondria rather than simple association between IPS-1 and DDX3 may be critical for the DDX3 function.

Evidence is accumulating that HCV checks many steps in the IFN-inducing pathway throughout the early and late infection stages, and suppresses IFN production by multiple means. Disruption of IPS-1 function by both NS3/4A and core protein may be crucial in HCV-infected Huh7.5 cells, even though the cells harbor dysfunctional RIG-I [46]. Type I IFN suppresses tumors by causing expression of p53 and other tumor-suppressing agents [47]. These unique features of the HCV core protein require further confirmation, and should be minded in investigation of HCV persistency, chronic infection and progression to cirrhosis and carcinoma.

Supporting Information

Figure S1 The IPS-1 complex. IPS-1 and HCV core bind C-terminal regions of DDX3. DDX3 captures dsRNA at the C-terminal domain. This figure is constructed from [11], [14] and [16].
Found at: doi:10.1371/journal.pone.0014258.s001 (0.41 MB TIF)

Figure S2 DDX3 enhances RIG-I-mediated IFN-β promoter activation induced by polyI:C. (A) DDX3 si-1 or control siRNA was transfected into HEK293 cells with reporter plasmids and RIG-I-expression plasmid or control plasmid (100 ng). After 48 hrs, cells were stimulated with polyI:C (20 μg/ml) with dextran for 4 hrs, and activation of the reporter p125luc was measured. (B) MDA5 (25 ng), IPS-1 (100 ng), DDX3 (100 ng), JFH1 core (50 ng) and/or p125 luc reporter (100 ng) plasmids were transfected with HEK293 cells. Cell lysates were prepared after 24 hrs, and luciferase activities measured. The results are representative of two independent experiments, each performed in triplicate.
Found at: doi:10.1371/journal.pone.0014258.s002 (0.17 MB TIF)

Figure S3 DDX3 colocalizes with IPS-1 on the mitochondria in Huh7.5.1 cells. HA-tagged DDX3 and FLAG-tagged IPS-1 were co-transfected into Huh7.5.1 cells. After 24 hrs, cells were fixed with formaldehyde and stained with anti-HA polyclonal and FLAG monoclonal Abs. Alexa488 (DDX3-HA) or Alexa633 antibody was used for second antibody. Mitochondria were stained with Mitotracker Red. A representative result from three independent experiments is shown.
Found at: doi:10.1371/journal.pone.0014258.s003 (0.92 MB TIF)

Acknowledgments

We thank Drs. Y. Matsuura (Osaka Univ.), Kyoko Mori (Okayama Univ.), and M. Sasai (Yale Univ.) for invaluable discussions. Thanks are also due to Drs. T. Ebihara, K. Funami, A. Matsuo, A. Ishii, and M. Shingai in our laboratory for their critical discussions.

Author Contributions

Conceived and designed the experiments: HO MM TS. Performed the experiments: HO MM. Analyzed the data: HO MM KS TS. Contributed reagents/materials/analysis tools: MI AW OT SA NK KS. Wrote the paper: HO TS.

References

1. Yoneyama M, Kikuchi M, Natsukawa T, Shinobu N, Imaizumi T, et al. (2004) The RNA helicase RIG-I has an essential function in double-stranded RNA-induced innate antiviral responses. Nat Immunol 5: 730–737.
2. Yoneyama M, Kikuchi M, Matsumoto K, Imaizumi T, Miyagishi M, et al. (2005) Shared and unique functions of the DExD/H-box helicases RIG-I, MDA5, and LGP2 in antiviral innate immunity. J Immunol 175: 2851–2858.
3. Kato H, Takeuchi O, Sato S, Yoneyama M, Yamamoto M, et al. (2006) Differential roles of MDA5 and RIG-I helicases in the recognition of RNA viruses. Nature 441: 101–105.
4. Kawai T, Takahashi K, Sato S, Coban C, Kumar H, et al. (2005) IPS-1, an adaptor triggering RIG-I- and Mda5-mediated type I interferon induction. Nat Immunol 6: 981–988.

5. Meylan E, Curran J, Hofmann K, Moradpour D, Binder M, et al. (2005) Cardif is an adaptor protein in the RIG-I antiviral pathway and is targeted by hepatitis C virus. Nature 437: 1167–1172.
6. Seth RB, Sun L, Ea CK, Chen ZJ (2005) Identification and characterization of MAVS, a mitochondrial antiviral signaling protein that activates NF-kappaB and IRF 3. Cell 122: 669–682.
7. Xu LG, Wang YY, Han KJ, Li LY, Zhai Z, et al. (2005) VISA is an adapter protein required for virus-triggered IFN-beta signaling. Mol Cell 19: 727–740.
8. Schroder M, Baran M, Bowie AG (2008) Viral targeting of DEAD box protein 3 reveals its role in TBK1/IKKepsilon-mediated IRF activation. Embo J 27: 2147–2157.
9. Soulat D, Bürckstümmer T, Westermayer S, Goncalves A, Bauch A, et al. (2008) The DEAD-box helicase DDX3X is a critical component of the TANK-binding kinase 1-dependent innate immune response. Embo J 27: 2135–2146.
10. Kravchenko VV, Mathison JC, Schwamborn K, Mercurio F, Ulevitch RJ (2003) IKKi/IKKepsilon plays a key role in integrating signals induced by pro-inflammatory stimuli. J Biol Chem 278: 26612–26619.
11. Oshiumi H, Sakai K, Matsumoto M, Seya T (2010) DEAD/H BOX 3 (DDX3) helicase binds the RIG-I adaptor IPS-1 to up-regulate IFN-beta inducing potential. Eur J Immunol 40: 940–948.
12. Chao CH, Chen CM, Cheng PL, Shih JW, Tsou AP, et al. (2006) A DEAD box RNA helicase with tumor growth-suppressive property and transcriptional regulation activity of the p21waf1/cip1 promoter, is a candidate tumor suppressor. Cancer Res 66: 6579–6588.
13. Rocak S, Linder P (2004) DEAD-box proteins: the driving forces behind RNA metabolism. Nat Rev Mol Cell Biol 5: 232–241.
14. Owsianka AM, Patel AH (1999) Hepatitis C virus core protein interacts with a human DEAD box protein DDX3. Virology 257: 330–340.
15. Angus AGN, Dalrymple D, Boulant S, McGivern DR, Clayton RF, et al. (2010) Requirement of cellular DDX3 for hepatitis C virus replication is unrelated to its interaction with the viral core protein. J Gen Virol 91: 122–132.
16. Ariumi Y, Kuroki M, Abe K, Dansako H, Ikeda M, et al. (2007) DDX3 DEAD-box RNA helicase is required for hepatitis C virus RNA replication. J Virol 81: 13922–13926.
17. Chang PC, Chi CW, Chau GY, Li FY, Tsai YH, et al. (2006) DDX3, a DEAD box RNA helicase, is deregulated in hepatitis virus-associated hepatocellular carcinoma and is involved in cell growth control. Oncogene 25: 1991–2003.
18. Schroder M (2010) Human DEAD-box protein 3 has multiple functions in gene regulation and cell cycle control and is a prime target for viral manipulation. Biochem Pharmacol 79: 297–306.
19. Ikeda M, Abe K, Dansako H, Nakamura T, Naka K, et al. (2005) Efficient replication of a full-length hepatitis C virus genome, strain O, in cell culture, and development of a luciferase reporter system. Biochem Biophys Res Commun 329: 1350–1359.
20. Lin W, Kim SS, Yeung E, Kamegaya Y, Blackard JT, et al. (2006) Hepatitis C virus core protein blocks interferon signaling by interaction with the STAT1 SH2 domain. J Virol 2006 Sep; 80(18): 9226–35.
21. Sasai M, Shingai M, Funami K, Yoneyama M, Fujita T, et al. (2006) NAK-associated protein 1 participates in both the TLR3 and the cytoplasmic pathways in type I IFN induction. J Immunol 177: 8676–8683.
22. Oshiumi H, Matsumoto M, Funami K, Akazawa T, Seya T (2003) TICAM-1, an adaptor molecule that participates in Toll-like receptor 3-mediated interferon-beta induction. Nat Immunol 4: 161–167.
23. Saito T, Owen DM, Jiang F, Marcotrigiano J, Gale M, Jr. (2008) Innate immunity induced by composition-dependent RIG-I recognition of hepatitis C virus RNA. Nature 454: 523–527.
24. Saito T, Hirai R, Loo YM, Owen D, Johnson CL, et al. (2007) Regulation of innate antiviral defenses through a shared repressor domain in RIG-I and LGP2. Proc Natl Acad Sci U S A 104: 582–587.
25. Matsumoto M, Funami K, Tanabe M, Oshiumi H, Shingai M, et al. (2003) Subcellular localization of Toll-like receptor 3 in human dendritic cells. J Immunol 171: 3154–3162.
26. Oshiumi H, Matsumoto M, Hatakeyama S, Seya T (2009) Riplet/RNF135, a RING finger protein, ubiquitinates RIG-I to promote interferon-beta induction during the early phase of viral infection. J Biol Chem 284: 807–817.
27. Schwer B, Ren S, Pietschmann T, Kartenbeck J, Kaehlcke K, et al. (2004) Targeting of hepatitis C virus core protein to mitochondria through a novel C-terminal localization motif. J Virol 78: 7958–7968.
28. Cheng G, Zhong J, Chisari FV (2006) Inhibition of dsRNA-induced signaling in hepatitis C virus-infected cells by NS3 protease-dependent and -independent mechanisms. Proc Natl Acad Sci U S A 103: 8499–8504.
29. Miyanari Y, Atsuzawa K, Usuda N, Watashi K, Hishiki T, et al. (2007) The lipid droplet is an important organelle for hepatitis C virus production. Nat Cell Biol 9: 1089–1097.
30. Mulhern O, Bowie AG (2010) Unexpected roles for DEAD-box protein 3 in viral RNA sensing pathways. Eur J Immunol 40: 933–935.
31. Li XD, Sun L, Seth RB, Pineda G, Chen ZJ (2005) Hepatitis C virus protease NS3/4A cleaves mitochondrial antiviral signaling protein off the mitochondria to evade innate immunity. Proc Natl Acad Sci U S A 102: 17717–17722.
32. Wang H, Kim S, Ryu WS (2009) DDX3 DEAD-Box RNA helicase inhibits hepatitis B virus reverse transcription by incorporation into nucleocapsids. J Virol 83: 5815–5824.
33. Yedavalli VS, Neuveut C, Chi YH, Kleiman L, Jeang KT (2004) Requirement of DDX3 DEAD box RNA helicase for HIV-1 Rev-RRE export function. Cell 119: 381–392.
34. Chuang RY, Weaver PL, Liu Z, Chang TH (1997) Requirement of the DEAD-Box protein ded1p for messenger RNA translation. Science 275: 1468–1471.
35. Mamiya N, Worman HJ (1999) Hepatitis C virus core protein binds to a DEAD box RNA helicase. J Biol Chem 274: 15751–15756.
36. Li K, Foy E, Ferreon JC, Nakamura M, Ferreon AC, et al. (2005) Immune evasion by hepatitis C virus NS3/4A protease-mediated cleavage of the Toll-like receptor 3 adaptor protein TRIF. Proc Natl Acad Sci U S A 102: 2992–2997.
37. Abe T, Kaname Y, Hamamoto I, Tsuda Y, Wen X, et al. (2007) Hepatitis C virus nonstructural protein 5A modulates the toll-like receptor-MyD88-dependent signaling pathway in macrophage cell lines. J Virol 81: 8953–8966.
38. Heim MH, Moradpour D, Blum HE (1999) Expression of hepatitis C virus proteins inhibits signal transduction through the Jak-STAT pathway. J Virol 73: 8469–8475.
39. Arnaud N, Dabo S, Maillard P, Budkowska A, Kalliampakou KI, et al. (2010) Hepatitic C virus controls interferon production through PKR activation. PLoS One 5: e10575.
40. Ploss A, Evans MJ, Gaysinskaya VA, Panis M, You H, et al. (2009) Human occludin is a hepatitis C virus entry factor required for infection of mouse cells. Nature 457: 882–886.
41. Satoh T, Kato H, Kumagai Y, Yoneyama M, Sato S, et al. (2010) LGP2 is a positive regulator of RIG-I- and MDA5-mediated antiviral responses. Proc Natl Acad Sci U S A 107: 1512–1517.
42. Ishikawa H, Ma Z, Barber GN (2009) STING regulates intracellular DNA-mediated, type I interferon-dependent innate immunity. Nature 461: 788–793.
43. Dixit E, Boulant S, Zhang Y, Lee ASY, Odendall C, et al. (2010) Peroxisomes are signaling platforms for antiviral innate immunity. Cell 141: 668–681.
44. Yasukawa K, Oshiumi H, Takeda M, Ishihara N, Yanagi Y, et al. (2009) Mitofusin 2 inhibits mitochondrial antiviral signaling. Sci Signal 2: ra47.
45. Scott I (2010) The role of mitochondria in the mammalian antiviral defense system. Mitochondrion 10: 316–320.
46. Binder M, Kochs G, Bartenschlager R, Lohmann V (2007) Hepatitis C virus escape from the interferon regulatory factor 3 pathway by a passive and active evasion strategy. Hepatology 46: 1365–1374.
47. Takaoka A, Yanai H, Kondo S, Duncan G, Negishi H, et al. (2005) Integral role of IRF-5 in the gene induction programme activated by Toll-like receptors. Nature 434: 243–249.

OPEN ACCESS Freely available online

PLoS one

The ESCRT System Is Required for Hepatitis C Virus Production

Yasuo Ariumi[1]*, Misao Kuroki[1], Masatoshi Maki[2], Masanori Ikeda[1], Hiromichi Dansako[1], Takaji Wakita[3], Nobuyuki Kato[1]

1 Department of Tumor Virology, Okayama University Graduate School of Medicine, Dentistry, and Pharmaceutical Sciences, Okayama, Japan, **2** Department of Applied Molecular Biosciences, Graduate School of Bioagricultural Sciences, Nagoya University, Nagoya, Japan, **3** Department of Virology II, National Institute of Infectious Diseases, Tokyo, Japan

Abstract

Background: Recently, lipid droplets have been found to be involved in an important cytoplasmic organelle for hepatitis C virus (HCV) production. However, the mechanisms of HCV assembly, budding, and release remain poorly understood. Retroviruses and some other enveloped viruses require an endosomal sorting complex required for transport (ESCRT) components and their associated proteins for their budding process.

Methodology/Principal Findings: To determine whether or not the ESCRT system is needed for HCV production, we examined the infectivity of HCV or the Core levels in culture supernatants as well as HCV RNA levels in HuH-7-derived RSc cells, in which HCV-JFH1 can infect and efficiently replicate, expressing short hairpin RNA or siRNA targeted to tumor susceptibility gene 101 (TSG101), apoptosis-linked gene 2 interacting protein X (Alix), Vps4B, charged multivesicular body protein 4b (CHMP4b), or Brox, all of which are components of the ESCRT system. We found that the infectivity of HCV in the supernatants was significantly suppressed in these knockdown cells. Consequently, the release of the HCV Core into the culture supernatants was significantly suppressed in these knockdown cells after HCV-JFH1 infection, while the intracellular infectivity and the RNA replication of HCV-JFH1 were not significantly affected. Furthermore, the HCV Core mostly colocalized with CHMP4b, a component of ESCRT-III. In this context, HCV Core could bind to CHMP4b. Nevertheless, we failed to find the conserved viral late domain motif, which is required for interaction with the ESCRT component, in the HCV-JFH1 Core, suggesting that HCV Core has a novel motif required for HCV production.

Conclusions/Significance: These results suggest that the ESCRT system is required for infectious HCV production.

Citation: Ariumi Y, Kuroki M, Maki M, Ikeda M, Dansako H, et al. (2011) The ESCRT System Is Required for Hepatitis C Virus Production. PLoS ONE 6(1): e14517. doi:10.1371/journal.pone.0014517

Editor: Gian Maria Fimia, INMI, Italy

Received May 6, 2010; **Accepted** December 15, 2010; **Published** January 11, 2011

Funding: This work was supported by a Grant-in-Aid for Scientific Research (C) from the Japan Society for the Promotion of Science (JSPS), by a Grant-in-Aid for Research on Hepatitis from the Ministry of Health, Labor, and Welfare of Japan, by the Viral Hepatitis Research Foundation of Japan, by the Kawasaki Foundation for Medical Science, Medical Welfare, by the Okayama Medical Foundation, and by Ryobi Teien Memory Foundation. MK was supported by a Research Fellowship from the JSPS for Young Scientists. The funders had no role in study design, data collection and analysis, decision to publish, or preparation of the manuscript.

Competing Interests: The authors have declared that no competing interests exist.

* E-mail: ariumi@md.okayama-u.ac.jp

Introduction

Hepatitis C virus (HCV) is a causative agent of chronic hepatitis, which progresses to liver cirrhosis and hepatocellular carcinoma. HCV is an enveloped virus with a positive single stranded 9.6 kb RNA genome, which encodes a large polyprotein precursor of approximately 3,000 amino acid residues. This polyprotein is cleaved by a combination of the host and viral proteases into at least 10 proteins in the following order: Core, envelope 1 (E1), E2, p7, nonstructural protein 2 (NS2), NS3, NS4A, NS4B, NS5A, and NS5B [1]. HCV Core, a highly basic RNA-binding protein, forms a viral capsid and is targeted to lipid droplets [2–6]. The Core is essential for infectious virion production [7]. NS5A, a membrane-associated RNA-binding phosphoprotein, is also involved in the assembly and maturation of infectious HCV particles [8,9]. Intriguingly, NS5A is a key regulator of virion production through the phosphorylation by casein kinase II [9]. Recently, lipid droplets have been found to be involved in an important cytoplasmic organelle for HCV production [4]. Indeed, NS5A is known to colocalize with the Core on lipid droplets [5], and the interaction between NS5A and the Core is critical for the production of infectious HCV particles [3]. However, the host factor involved in HCV assembly, budding, and release remains poorly understood.

Budding is an essential step in the life cycle of enveloped viruses. Endosomal sorting complex required for transport (ESCRT) components and associated factors, such as tumor susceptibility gene 101 (TSG101, a component of ESCRT-I), charged multivesicular body protein 4b (CHMP4b, a component of ESCRT-III), and apoptosis-linked gene 2 interacting protein X (ALIX, a TSG101- and CHMP4b-binding protein), have been found to be involved in membrane remodeling events that accompany endosomal protein sorting, cytokinesis, and the budding of several enveloped viruses, such as human immunodeficiency virus type 1 (HIV-1) [10–12]. The ESCRT complexes I, II, and III are sequentially, or perhaps concentrically recruited to the endosomal membrane to sequester

cargo proteins and drive vesicularization into the endosome. Finally, ESCRT-III recruits Vps4 (two isoforms, Vps4A and Vps4B), a member of the AAA-family of ATPase that disassembles and thereby terminates and recycles the ESCRT machinery.

Since HCV is also an enveloped RNA virus, we hypothesized that the ESCRT system might be required for HCV production. To test this hypothesis, we examined the release of HCV Core into culture supernatants from cells rendered defective for ESCRT components by RNA interference. The results provide evidence that the ESCRT system is required for HCV production.

Materials and Methods

Cell Culture

293FT cells (Invitrogen, Carlsbad, CA) were cultured in Dulbecco's modified Eagle's medium (DMEM; Invitrogen) supplemented with 10% fetal bovine serum (FBS). The HuH-7-derived cell line, RSc cured cells that cell culture-generated HCV-JFH1 (JFH1 strain of genotype 2a) [13] could infect and effectively replicate [14–16] and OR6c and OR6 cells harboring the genome-length HCV-O RNA with luciferase as a reporter were cultured in DMEM with 10% FBS as described previously [17,18].

Plasmid Construction

To construct pcDNA3-FLAG-Alix, a DNA fragment encoding Alix was amplified from total RNAs derived from RSc cells by RT-PCR using the follwing pairs of primers: Forward 5′-CGGGATCCAAGATGGCGACATTCATCTCGGT-3′ and reverse 5′-CCGGCGGCCGCTTACTGCTGTGGATAGTAAG-3′. The obtained DNA fragment was subcloned into *Bam*HI-*Not*I of pcDNA3-FLAG vector [19], and the nucleotide sequences were determined by Big Dye termination cycle sequencing using an ABI Prism 310 genetic analyzer (Applied Biosystems, Foster City, CA, USA). The plasmid of pJRN/3-5B was based on pJFH1 [13] and was constructed as previously described [20].

RNA synthesis, RNA transfection, and Selection of G418-resistant cells

Plasmid pJRN/3-5B were linearized by *Xba*I and used for the RNA synthesis with the T7 MEGAScript kit (Ambion, Austin, TX). *In vitro* transcribed RNA was transfected into OR6c cells by electroporation [17,18]. The transfected cells were selected in culture medium containing G418 (0.3 mg/ml) for 3 weeks. We referred to them as OR6c/JRN 3-5B cells.

Immunofluorescence and Confocal Microscopic Analysis

Cells were fixed in 3.6% formaldehyde in phosphate-buffered saline (PBS) and permeabilized in 0.1% Nonidet P-40 (NP-40) in PBS at room temperature as previously described [21]. Cells were incubated with anti-HCV Core antibody (CP-9 and CP-11 mixture; Institute of Immunology, Tokyo, Japan), anti-Myc-Tag antibody (PL14; Medical & Biological Laboratories, MBL, Nagoya, Japan), anti-Alix antibody (Covalab, Villeurbanne, France), and/or anti-FLAG polyclonal antibody (Sigma, St. Louis, MO) at a 1:300 dilution in PBS containing 3% bovine serum albumin (BSA) at 37°C for 30 min. Cells were then stained with fluorescein isothiocyanate (FITC)-conjugated anti-rabbit antibody (Jackson ImmunoResearch, West Grove, PA) or anti-Cy3-conjugated anti-mouse antibody (Jackson ImmunoResearch) at a 1:300 dilution in PBS containing BSA at 37°C for 30 min. Lipid droplets and nuclei were stained with BODIPY 493/503 (Molecular Probes, Invitrogen) and DAPI (4′,6′-diamidino-2-phenylindole), respectively. Following extensive washing in PBS, cells were mounted on slides using a mounting media of 90% glycerin/10% PBS with 0.01% *p*-phenylenediamine added to reduce fading. Samples were viewed under a confocal laser-scanning microscope (LSM510; Zeiss, Jena, Germany).

RNA Interference

The following siRNAs were used: human TSG101 (siGENOME SMARTpool M-003549-01-0005 and 5′-CCUCCAGUCUUCUCUCGUCUU-3′ sense, 5′-GACGAGAGAAGACUGGAGGUU-3′ antisense), human Alix/PDCD6IP (siGENOME SMARTpool M-004233-02-0005), human Vps4B (siGENOME SMARTpool M-013119-02-0005), human CHMP4b (siGENOME SMARTpool M-018075-00-0005), and siGENOME Non-Targeting siRNA Pool#1 (D-001206-13-05) (Dharmacon, Thermo Fisher Scientific, Waltham, MA) as a control. siRNAs (50 nM final concentration) were transiently transfected into either RSc cells [14–16] or OR6 cells [17,18] using Oligofectamine (Invitrogen) according to the manufacturer's instructions. Oligonucleotides with the following sense and antisense sequences were used for the cloning of short hairpin (sh) RNA-encoding sequences against TSG101, Alix, Vps4B, or CHMP4b in lentiviral vector: TSG101i, 5′-GATCCCC GGAGGAAATGGATCGTGCCTTCAAGAGAGGCACGATCCATTTCCTCCTTTTTGGAAA-3′ (sense), 5′-AGCTTTTCCAAAAAGGAGGAAATGGATCGTGCCTCTCTTGAAGGCACGATCCATTTCCTCCGGG-3′ (antisense); Alixi, 5′-GATCCCC GGAGGTGTTCCCTGTCTTGTTCAAGAGACAAGACAGGGAACACCTCCTTTTTGGAAA-3′ (sense), 5′-AGCTTTTCCAAAAAGGAGGTGTTCCCTGTCTTGTCTCTTGAACAAGACAGGGAACACCTCCGGG-3′ (antisense); Vps4Bi, 5′-GATCCCC GGAGAATCTGATGATCCTGTTCAAGAGACAGGATCATCAGATTCTCCTTTTTGGAAA-3′ (sense), 5′-AGCTTTTCCAAAAAGGAGAATCTGATGATCCTGTCTCTTGAACAGGATCATCAGATTCTCCGGG-3′ (antisense); CHMP4bi, 5′-GATCCCC GAGGAGGACGACGACATGATTCAAGAGATCATGTCGTCGTCCTCCTCTTTTTGGAAA-3′ (sense), 5′-AGCTTTTCCAAAAAGAGGAGGACGACGACATGATCTCTTGAATCATGTCGTCGTCCTCCTCGGG-3′ (antisense); Broxi, 5′-GATCCCCGGATGACAGTACTAAACCCTTCAAGAGAGGGTTTAGTACTGTCATCCTTTTTGGAAA-3′ (sense), 5′-AGCTTTTCCAAAAAGGATGACAGTACTAAACCCTCTCTTGAAGGGTTTAGTACTGTCATCCGGG-3′ (antisense). The oligonucleotides above were annealed and subcloned into the *Bgl*II-*Hin*dIII site, downstream from an RNA polymerase III promoter of pSUPER [22], to generate pSUPER-TSG101i, pSUPER-Alixi, pSUPER-Vps4Bi, and pSUPER-CHMP4bi, respectively. To construct pLV-TSG101i, pLV-Alixi, pLV-Vps4Bi, and pLV-CHMP4bi, the *Bam*HI-*Sal*I fragments of the corresponding pSUPER plasmids were subcloned into the *Bam*HI-*Sal*I site of pRDI292 [23], an HIV-1-derived self-inactivating lentiviral vector containing a puromycin resistant marker allowing for the selection of transduced cells, respectively.

Lentiviral Vector Production

The vesicular stomatitis virus (VSV)-G-pseudotyped HIV-1-based vector system has been described previously [24–26]. The lentiviral vector particles were produced by transient transfection of the second-generation packaging construct pCMV-ΔR8.91 [24–26] and the VSV-G-envelope-expressing plasmid pMDG2 as well as pRDI292 into 293FT cells with FuGene6 (Roche Diagnostics, Basel, Switzerland).

HCV Infection Experiments

The supernatants was collected from cell culture-generated HCV-JFH1 [13]-infected RSc cells [14–16] at 5 days post-

infection and stored at −80°C after filtering through a 0.45 μm filter (Kurabo, Osaka, Japan) until use. For infection experiments with HCV-JFH1 virus, RSc cells (1×10^5 cells/well) were plated onto 6-well plates and cultured for 24 hours (hrs). Then, we infected the cells with 50 μl (equivalent to a multiplicity of infection [MOI] of 0.1) of inoculum. The culture supernatants were collected and the levels of HCV Core were determined by enzyme-linked immunosorbent assay (ELISA) (Mitsubishi Kagaku Bio-Clinical Laboratories, Tokyo, Japan). Total RNA was isolated from the infected cellular lysates using RNeasy mini kit (Qiagen, Hilden, Germany) for quantitative RT-PCR analysis of intracellular HCV RNA. The infectivity of HCV in the culture supernatants was determined by a focus-forming assay at 48 hrs post-infection. The HCV infected cells were detected using anti-HCV Core antibody (CP-9 and CP-11). Intracellular HCV infectivity was determined by a focus-forming assay at 48 hrs post-inoculation of lysates by repeated freeze and thaw cycles (three times).

Quantitative RT-PCR Analysis

The quantitative RT-PCR analysis for HCV RNA was performed by real-time LightCycler PCR (Roche) as described previously [17,18]. We used the following forward and reverse primer sets for the real-time LightCycler PCR: TSG101, 5′-ATGGCGGTGTCGGAGAGCCA-3′ (forward), 5′-AACAGGTTTGAGATCTTTGT-3′ (reverse); Alix, 5′-ATGGCGACATTCATCTCGGT-3′ (forward), 5′-TACTGGGCCTGCTCTTCCCC-3′ (reverse); Vps4B, 5′-ATGTCATCCACTTCGCCCAA-3′ (forward), 5′-ATACTGCACAGCATGCTGAT-3′ (reverse); CHMP4b, 5′-ATGTCGGTGTTCGGGAAGCT-3′ (forward), 5′-ATCTCTTCCGTGTCCCGCAG-3′ (reverse); Brox, 5′-ATGACCCATTGGTTTCATAG-3′ (forward), 5′-CCTGGATGACCTCAAGTCAT-3′ (reverse); β-actin, 5′-TGACGGGGTCACCCACACTG-3′ (forward), 5′-AAGCTGTAGCCGCGCTCGGT-3′ (reverse); and HCV-JFH1, 5′-AGAGCCATAGTGGTCTGCGG-3′ (forward), 5′-CTTTCGCAACCCAACGCTAC-3′ (reverse).

MTT Assay

Cells (5×10^3 cells/well) were plated onto 96-well plates and cultured for 24, 48 or 72 hrs, then, subjected to the colorimetric 3-(4,5-dimethylthiazol-2-yl)-2,5-diphenyltetrazolium bromid (MTT) assay according to the manufacturer's instructions (Cell proliferation kit I, Roche). The absorbance was read using a microplate reader (Multiskan FC, Thermo Fisher Scientific) at 550 nm with a reference wavelength of 690 nm.

Renilla Luciferase (RL) Assay

OR6 cells (1.5×10^4 cells/well) [17,18] were plated onto 24-well plates and cultured for 24 hrs. The cells were transfected with siRNAs (50 nM) using Oligofectamine and incubated for 72 hrs, then, subjected to the RL assay according to the manufacturer's instructions (Promega, Madison, WI). A lumat LB9507 luminometer (Berthold, Bad Wildbad, Germany) was used to detect RL activity.

Western Blot Analysis

Cells (2×10^5 cells/well) were plated onto 6-well plates and cultured for 24 or 48 hrs. Cells were lysed in buffer containing 50 mM Tris-HCl (pH 8.0), 150 mM NaCl, 4 mM EDTA, 1% NP-40, 0.1% sodium dodecyl sulfate (SDS), 1 mM dithiothreitol (DTT) and 1 mM phenylmethylsulfonyl fluoride (PMSF). Supernatants from these lysates were subjected to SDS-polyacrylamide gel electrophoresis, followed by immunoblot analysis using anti-TSG101 antibody (BD Transduction Laboratories, San Jose, CA), anti-Alix antibody, anti-Vps4B antibody (Abnova, Taipei, Taiwan) (A302-078A; Bethyl Laboratories, Montgomery, TX), anti-CHMP4B antibody (sc-82557; Santa Cruz Biotechnology, Santa Cruz, CA), anti-HCV Core antibody, anti-β-actin antibody (Sigma), anti-Myc-Tag antibody, anti-FLAG antibody (M2; Sigma), anti-Chk2 antibody (DCS-273; MBL), anti-heat shock protein (HSP) 70 antibody (BD), Living Colors A.v. monoclonal antibody (JL-8; Clontech, Mountain View, CA), anti-HCV NS5A monoclonal antibody (no. 8926; a generous gift from A Takamizawa, The Research Foundation for Microbial Diseases of Osaka University, Japan), or anti-HCV NS5A polyclonal antibody (a generous gift from K Shimotohno, Chiba Institute of Technology, Chiba, Japan).

Immunoprecipitation Analysis

Cells were lysed in buffer containing 10 mM Tris-HCl (pH 8.0), 150 mM NaCl, 1% NP-40, 1 mM PMSF, and protease inhibitor cocktail containing 104 μM 4-(2-aminoethyl)benzenesulfonyl fluoride hydrochloride, 80 nM aprotinin, 2.1 μM leupeptin, 3.6 μM bestatin, 1.5 μM pepstatin A, and 1.4 μM E-64 (Sigma). Lysates were pre-cleaned with 30 μl of protein-G-Sepharose (GE Healthcare Bio-Sciences). Pre-cleaned supernatants were incubated with 5 μl of Living Colors A.v. monoclonal antibody or anti-FLAG antibody at 4°C for 1 hr. Following absorption of the precipitates on 30 μl of protein-G-Sepharose resin for 1 hr, the resin was washed four times with 700 μl lysis buffer. Proteins were eluted by boiling the resin for 5 min in 1× Laemmli sample buffer. The proteins were then subjected to SDS-PAGE, followed by immunoblotting analysis using either anti-FLAG antibody, Living Colors A.v. monoclonal antibody or anti-HCV Core antibody.

Statistical Analysis

Statistical comparison of the infectivity of HCV in the culture supernatants between the knockdown cells and the control cells was performed using the Student's *t*-test. *P* values of less than 0.05 were considered statistically significant. All error bars indicate standard deviation.

Results

The ESCRT system is required for HCV production

To investigate the potential role(s) of the ESCRT system in the HCV life cycle, we first used lentiviral vector-mediated RNA interference to stably knockdown the ESCRT components, including TSG101, Alix, Vps4B, or CHMP4b in HuH-7-derived RSc cured cells that cell-culture-generated HCVcc (HCV-JFH1, genotype 2a) [13] could infect and effectively replicate [14–16]. We used puromycin-resistant pooled cells 10 days after the lentiviral transduction in all experiments. Western blot and real-time LightCycler RT-PCR analyses for TSG101, Alix, Vps4B, or CHMP4b demonstrated a very effective knockdown of each ESCRT component in RSc cells transduced with lentiviral vectors expressing the corresponding shRNAs (Fig. 1A–E). Importantly, we noticed that the depletion of ESCRT components did not affect the levels of several cellular proteins, including HSP70, Chk2, and b-actin (Fig. 1A). To test the cell toxicity of each shRNA, we examined colorimetric MTT assay. In this context, we demonstrated that the shRNAs did not affect the cell viabilities (Fig. 1F). We next examined the levels of HCV Core and the infectivity of HCV in the culture supernatants as well as the level of HCV RNA in the TSG101, Alix, Vps4B, or CHMP4b stable knockdown RSc cells 97 h after HCV-JFH1 infection at an MOI of 0.1. The results showed that the release of HCV Core into the culture supernatants

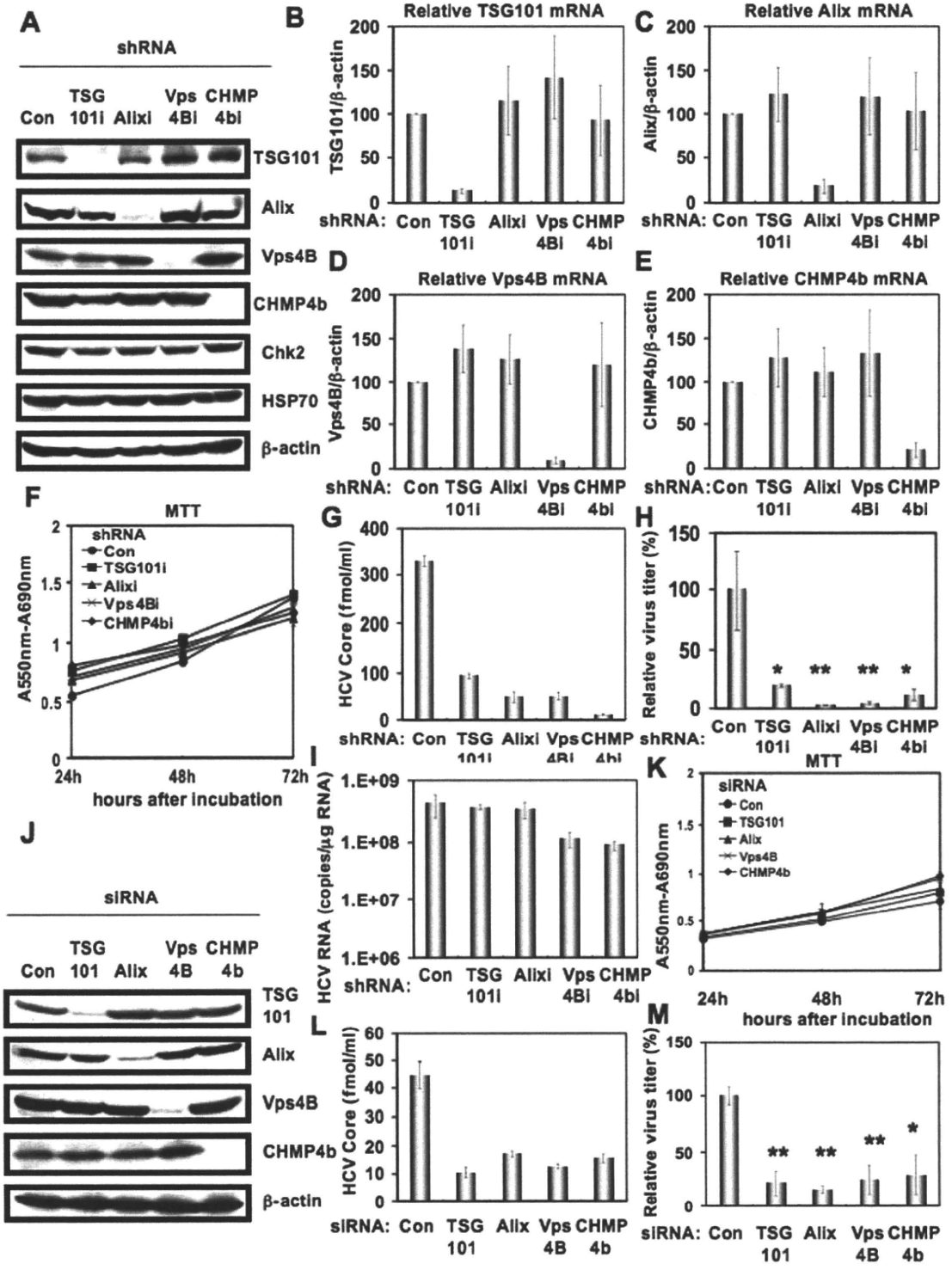

Figure 1. ESCRT components are required for the infectious HCV production. (A) Inhibition of TSG101, Alix, Vps4B, or CHMP4b protein expression by shRNA-producing lentiviral vectors. The results of the Western blot analysis of cellular lysates with anti-TSG101, anti-Alix, anti-Vps4B, anti-CHMP4b, anti-Chk2, anti-HSP70, or anti-β-actin antibody in RSc cells expressing shRNA targeted to TSG101 (TSG101i), Alix (Alixi), Vps4B (Vps4Bi), or CHMP4b (CHMP4bi) as well as in RSc cells transduced with a control lentiviral vector (Con) are shown. Real-time LightCycler RT-PCR for TSG101 (B), Alix (C), Vps4B (D), or CHMP4b mRNA (E) was performed as well as for β-actin mRNA in triplicate. Each mRNA level was calculated relative to the level in RSc cells transduced with a control lentiviral vector (Con) which was assigned as 100%. Error bars in this panel and other figures indicate standard deviations. (F) MTT assay of each knockdown RSc cells at the indicated time. (G) The levels of HCV Core in the culture supernatants from the stable knockdown RSc cells 97 h after inoculation of HCV-JFH1 at an MOI of 0.1 were determined by ELISA. Experiments were done in triplicate and columns represent the mean Core protein levels. (H) The infectivity of HCV in the culture supernatants from the stable knockdown RSc cells 97 hrs after inoculation of HCV-JFH1 at an MOI of 0.1 was determined by a focus-forming assay at 48 hrs post-infection. Experiments were done in triplicate and each virus titer was calculated relative to the level in RSc cells transduced with a control lentiviral vector (Con) which was assigned as 100%. Asterisks indicate significant differences compared to the control treatment. *$P<0.05$; **$P<0.01$. (I) The level of intracellular genome-length HCV-JFH1 RNA in the cells at 97 hrs post-infection was monitored by real-time LightCycler RT-PCR. Results

from three independent experiments are shown. (J) Inhibition of TSG101, Alix, Vps4B, or CHMP4b protein expression by 72 hrs after transient transfection of RSc cells with a pool of control siRNA (Con) or a pool of siRNA specific for Alix, Vps4B, or CHMP4b (50 nM). The results of the Western blot analysis of cellular lysates with anti-TSG101, anti-Alix, anti-Vps4B, anti-CHMP4b, or anti-β-actin antibody is shown. (K) MTT assay of each knockdown RSc cells at the indicated time. (L) The levels of HCV Core in the culture supernatants were determined by ELISA 24 hrs after inoculation of HCV-JFH1. RSc cells were transiently transfected with a pool of control siRNA (Con) or a pool of siRNA specific for TSG101, Alix, Vps4B, or CHMP4b (50 nM). At 48 hrs after transfection, the cells were inoculated with HCV-JFH1 at an MOI of 5 and incubated for 2 hrs. Then, culture medium was changed and incubated for 22 hrs. Experiments were done in triplicate and each Core level was calculated relative to the level in the culture supernatants from the control cells and indicated below. (M) The infectivity of HCV in the culture supernatants from the transient knockdown RSc cells 24 hrs after inoculation of HCV-JFH1 at an MOI of 5 was determined by a focus-forming assay at 48 hrs post-infection. Experiments were done in triplicate and each virus titer was calculated relative to the level in RSc cells transfected with a control siRNA (Con) which was assigned as 100%. Asterisks indicate significant differences compared to the control treatment. *$P<0.05$; **$P<0.01$.

doi:10.1371/journal.pone.0014517.g001

was significantly suppressed in these knockdown cells after HCV-JFH1 infection (Fig. 1G). Importantly, the infectivity of HCV in the culture supernatants was also significantly suppressed in these knockdown cells (Fig. 1H), while the RNA replication of HCV-JFH1 was not affected in the TSG101 or Alix knockdown cells and was somewhat decreased in the Vps4B and CHMP4b knockdown cells (Fig. 1I). This suggested that the ESCRT system is associated with infectious HCV production. To further confirm whether or not the ESCRT system is involved in HCV production, we analyzed the single-round HCV replication. For this, we used RSc cells transiently transfected with a pool of siRNAs specific for TSG101, Alix, Vps4B, or CHMP4b as well as a pool of control siRNAs (Con) following HCV infection. In spite of very effective knockdown of each ESCRT component (Fig. 1J), we demonstrated that the siRNAs did not affect the cell viabilities by MTT assay (Fig. 1K). Consistent with our finding using the stable knockdown cells, we observed that the release of HCV Core or the infectivity of HCV into the culture supernatants was significantly suppressed in these transient knockdown cells 24 hrs after HCV-JFH1 infection (Fig. 1L and 1M). Furthermore, we examined the effect of siRNA specific for TSG101, Alix, Vps4B, or CHMP4b in HCV RNA replication using the subgenomic JFH1 replicon, JRN/3-5B, encoding *Renilla* luciferase gene for monitoring the HCV RNA replication in HuH-7-derived OR6c JRN/3-5B cells (Fig. 2A and 2B) or an OR6 assay system, which was developed as a luciferase reporter assay system for monitoring genome-length HCV RNA replication (HCV-O, genotype 1b) in HuH-7-derived OR6 cells (Fig. 2C) [17,18]. The results showed that these siRNAs could not affect HCV RNA replication as well as the levels of intracellular NS5A proteins (Fig. 2A–C). Although we have demonstrated that the ESCRT system is required for production of extracellular infectious HCV particles, it is not clear whether or not these findings are associated with the assembly of intracellular infectious particles. To test this point, infectivity of intracellular infectious particles was analyzed following lysis of HCV-JFH1-infected knockdown cells by repetitive freeze and thaw. Consequently, we did not observe any significant effects of siRNAs on the accumulation of intracellular infectious HCV-JFH1, while the accumulation of extracellular HCV was significantly suppressed in these knockdown cells (Fig. 2D and 2E), indicating that inhibition of the ESCRT system does not block the accumulation of intracellular infectious HCV particles. Furthermore, Western blot analysis of cell lysates demonstrated that the level of intracellular HCV Core and NS5A was not affected in these knockdown cells 72 hrs post-infection (Fig. 2F). Thus, we conclude that the ESCRT system is not required for the assembly of infectious particles but the ESCRT system is required for late step of HCV production.

HCV Core can target into lipid droplets in the ESCRT knockdown cells

Since lipid droplets have been shown to be involved in an important cytoplasmic organelle for HCV production [4], we performed immunofluorescence and confocal microscopic analyses to determine whether or not HCV Core misses localization into lipid droplets in the ESCRT knockdown cells. We found that the Core was targeted into lipid droplets even in TSG101 knockdown, Alix knockdown, Vps4B knockdown, or CHMP4b knockdown RSc cells as well as in the control RSc cells after HCV infection (Fig. 3). This suggests that the ESCRT system plays a role in the late step after the Core is targeted into lipid droplets in the HCV life cycle.

HCV Core interacts with CHMP4b

To determine whether or not HCV Core can interact with ESCRT component(s), we examined their subcellular localization by confocal laser scanning microscopy. Consequently, the Core mostly colocalized with CHMP4b-green fluorescent protein (GFP) or FLAG-tagged CHMP4b in the perinuclear region of 293FT cells coexpressing them (Fig. 4A and 4B), while the CHMP4b-GFP alone was slightly diffused in the cytoplasm (Fig. 4A), indicating the recruitment of CHMP4b in the Core-expressing area. Importantly, we observed similar partial colocalization in HCV-JFH1-infected RSc cells expressing CHMP4b-GFP (Fig. 4C), whereas the CHMP4b-GFP alone was diffused in the cytoplasm in the uninfected RSc cells (Fig. 4C), suggesting the interaction of HCV Core with CHMP4b. Unfortunately, we failed to observe endogenous CHMP4b using several commercially available anti-CHMP4b antibody (data not shown). Consistent with a previous report that interaction between HCV Core and NS5A is critical for HCV production [3], we found the partial colocalization of NS5A with CHMP4b-GFP as well as the colocalization of Core with CHMP4b-GFP in HCV-JFH1-infected RSc cells (Fig. 4C). Then, we examined whether or not HCV Core can bind to CHMP4b by immunoprecipitation analysis. 293FT cells transfected with 4 mg of pCHMP4b-GFP, pEGFP C3 (Clontech), pcDNA3-FLAG [19], pcDNA3-FLAG-Alix or pFLAG-CHMP4b and RSc cells 5 days after inoculation of HCV-JFH1 at an MOI of 4 were lysed and performed immunoprecipitation of lysate mixtures of HCV-JFH1-infected RSc cells and 293FT cells expressing CHMP4b-GFP, GFP alone, FLAG-CHMP4b or FLAG-epitope alone with anti-FLAG or anti-GFP antibody. Consequently, we observed that the Core but not the NS5A could bind to FLAG-CHMP4b (Fig. 4D). However, the Core was not immunoprecipitated with anti-FLAG antibody using the lysate mixtures of HCV-JFH1-infected RSc cell lysates and 293FT cells expressing FLAG-epitope alone or FLAG-Alix (Fig. 4D). Furthermore, the Core was coimmunoprecipitated with CHMP4b-GFP but not GFP when lysate mixtures of HCV-JFH1-infected RSc cells and 293FT cells expressing CHMP4b-GFP or GFP alone were used (Fig. 4D). In contrast, we failed to observe the marked colocalization of HCV-JFH1 Core with Myc-tagged TSG101 in HCV-JFH1-infected RSc cells expressing Myc-TSG101 or endogenous Alix in HCV-JFH1-infected RSc cells (Fig. 5A). Thus, we concluded that the HCV Core was associated with CHMP4b.

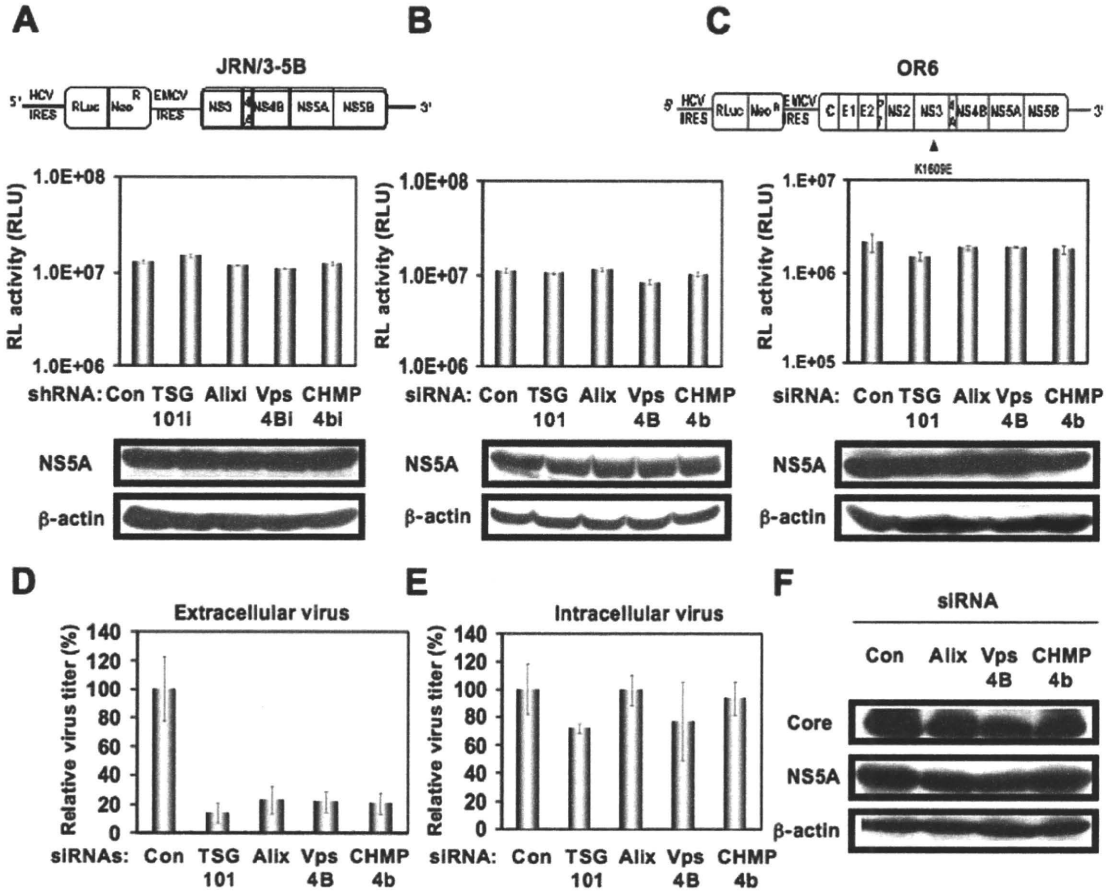

Figure 2. ESCRT system is not required for HCV RNA replication and assembly of intracellular infectious HCV. (A) Schematic gene organization of subgenomic JFH1 (JRN/3-5B) RNA encoding *Renilla* luciferase gene. Renilla luciferase gene (RLuc) is depicted as a box and is expressed as a fusion protein with Neo. The HCV RNA replication level in each ESCRT knockdown OR6c JRN/3-5B cells by lentiviral vector-mediated RNA interference (shRNA) was monitored by RL assay. The RL activity (RLU) is shown. The results shown are means from three independent experiments. (B) 72 hrs after the transfection of OR6c JRN/3-5B polyclonal cells with each of the siRNA (50 nM), the HCV RNA replication level was monitored by RL assay as described in (A). (C) Schematic gene organization of genome-length HCV-O RNA encoding *Renilla* luciferase gene. The position of an adaptive mutation, K1609E, is indicated by a triangle. 72 hrs after the transfection of OR6 cells with each of the siRNA (50 nM), the HCV RNA replication level was monitored by RL assay as described in (A). (D) The infectivity of HCV in the culture supernatants from the transient knockdown RSc cells 24 hrs after inoculation of HCV-JFH1 at an MOI of 2 was determined by a focus-forming assay at 48 hrs post-infection. Experiments were done in triplicate and each virus titer was calculated relative to the level in RSc cells transfected with a control siRNA (Con) which was assigned as 100%. (E) Intracellular HCV infectivity was determined by a focus-forming assay at 48 hrs post-inoculation of lysates by repeated freeze and thaw cycles as described in (D). (F) RSc cells were transiently transfected with a pool of control siRNA (Con) or a pool of siRNA specific for Alix, Vps4B, or CHMP4b (50 nM). At 24 hrs after the transfection, the cells were inoculated with HCV-JFH1 at an MOI of 0.2 and incubated for 48 hrs. Then, culture medium was changed and incubated for 24 hours. Western blotting of cell lysates 72 hrs post-infection with anti-β-actin, anti-HCV NS5A, or anti-HCV Core antibody is shown.
doi:10.1371/journal.pone.0014517.g002

Finally, we examined the subcellular localization of HCV Core and Brox, a novel farnesylated Bro1 domain-containing protein, since Brox was recently identified as a CHMP4-binding protein [27]. In this context, the Core partially colocalized with GFP-Brox in 293FT cells coexpressing of HCV Core and GFP-Brox (Fig. 5B). Importantly, we observed similar partial colocalization in HCV-JFH1-infected RSc cells expressing GFP-Brox (Fig. 5C). On the other hand, the CHMP4b-GFP alone was diffused in the cytoplasm of uninfected RSc cells (Fig. 5C). To examine the potential role of Brox in HCV life cycle, we established the Brox knockdown RSc cells by lentiviral vector expressing shRNA targeted to Brox (Fig. 5D). Consequently, we found that the release of HCV Core or the infectivity of HCV into the culture supernatants was significantly suppressed in the Brox knockdown cells 4 days after HCV-JFH1 infection (Fig. 5E and 5F), while the RNA replication of HCV-JFH1 was marginally affected in the knockdown cells (Fig. 5G) in spite of the very effective knockdown of Brox mRNA (Fig. 5D), suggesting that Brox is also required for the infectious HCV production.

Discussion

In this study, we have demonstrated that the ESCRT system is required for infectious HCV production, and that HCV Core but not NS5A binds to CHMP4b, a component of ESCRT-III. Although RNA replication of HCV-JFH1 was not affected in the TSG101 knockdown or the Alix knockdown cells, the infectivity of HCV in the culture supernatants was significantly suppressed in these knockdown cells after HCV-JFH1 infection (Fig. 1G and 1H). Furthermore, siRNA targeted to TSG101, Alix, Vps4B, or CHMP4b significantly suppressed HCV Core level or the infectivity of HCV in the culture supernatants (Fig. 1L, 1M, and

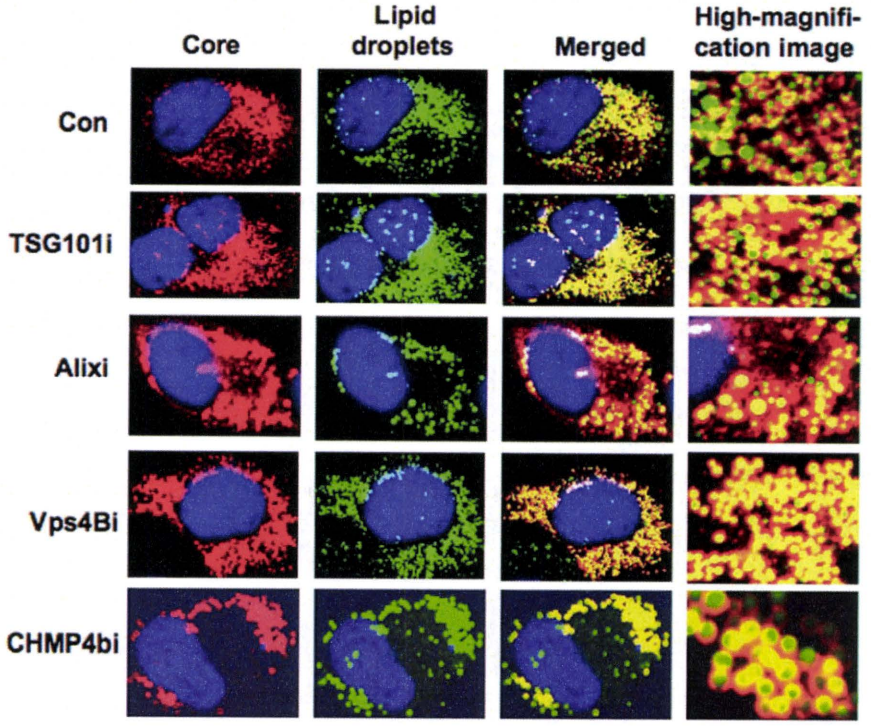

Figure 3. HCV Core is targeted to lipid droplets even in the ESCRT knockdown cells. The RSc cells transduced with a control lentiviral vector (Con), the TSG101 knockdown (TSG101i), the Alix knockdown (Alixi), the Vps4B knockdown (Vps4Bi), or the CHMP4b knockdown (CHMP4bi) cells were infected with HCV-JFH1. Cells were fixed 60 hrs post-infection and were then examined by confocal laser scanning microscopy. Cells were stained with anti-HCV Core (CP-9 and CP-11 mixture) and were then visualized with Cy3 (red). Lipid droplets and nuclei were stained with BODIPY 493/503 (green) and DAPI (blue), respectively. Images were visualized using confocal laser scanning microscopy. Colocalization is shown in yellow (Merged).
doi:10.1371/journal.pone.0014517.g003

2D), while the siRNA did not affect intracellular HCV Core level (Fig. 2E and 2F). Accordingly, we noticed some discrepancy that shRNA targeted to Vps4B or CHMP4b somewhat decreased intracellular HCV RNA replication (Fig. 1I), whereas siRNA targeted to TASG101, Alix, Vps4B or CHMP4b did not affect the RNA replication of subgenomic replicon of JFH1 (Fig. 2A and 2B). Furthermore, siRNAs targeted to TSG101, Alix, Vps4B, or CHMP4b did not affect HCV-O (genotype 1b) RNA replication using the OR6 assay system [17,18] (Fig. 2C), indicating that the ESCRT system is unrelated to the HCV RNA replication of genotype 1b. Thus, we suggested that the ESCRT system is not significant for HCV RNA replication. Within the family *Flaviviridae*, NS3 of the Japanese encephalitis virus (JEV) is also known to interact with TSG101 and microtubules, suggesting their potential roles in JEV assembly [28]. Accordingly, HCV NS3 has been involved in HCV particle assembly and infectivity [29,30]. However, whether HCV NS3 or another HCV protein binds to TSG101 remains to be investigated. At least, we did not observe the interaction between HCV NS5A and CHMP4b (Fig. 4D), Alix (Fig. 4D), TSG101, or Vps4B (data not shown).

Efficient enveloped virus release requires *cis*-acting viral late domains (L-domains), including P(T/S)AP, YPXnL (where X is any amino acid), and PPXY amino acid L-domain motif that are found in the structural proteins of other enveloped viruses [10,11]. Unlike the case with these enveloped viruses, we failed to find the three types of conserved viral L-domain motif in the HCV-JFH1 Core (data not shown). Nevertheless, we observed that the Core bound to CHMP4b, whereas NS5A did not (Fig. 4D), suggesting that the Core has a novel motif required for the HCV production. In this regard, Blanchard *et al.* reported that the aspartic acid at position 111 in the Core is crucial for virus assembly [31]. Interestingly, the conversion of the aspartic acid into alanine at amino acid 111 (PTDP to PTAP), which creates the PTAP L-domain motif, enhanced the release of HCV Core in the cell culture medium (a 2.5-fold increase) compared with the wild-type Core [31]. In contrast, Klein *et al.* demonstrated that the D111A mutation in the Core had no effect on HCV capsid assembly [32]. Furthermore, Murray *et al* found that serine 99, a putative phosphorylation site, in the Core was essential for infectious virion production [7]. In any event, the Core motif that is needed for interaction with the ESCRT components remains to be identified.

Ubiquitin modification of viral protein has been implicated in virion egress as well as in protein turnover. Indeed, the ubiquitin/proteasome system is required for the retrovirus budding machinery, since proteasome inhibition interferes with retroviral Gag polyprotein processing, release, and maturation. The ubiquitin modification of the HIV-1 p6 domain of Gag enhances TSG101 binding [12]. In the case of HCV Core, proteasomal degradation of the Core is mediated by two distinct mechanisms [33–36]. E6AP E3 ubiquitin ligase mediates ubiquitylation and degradation of the Core [34]. In contrast, proteasome activator PA28γ (11S regulator γ), an HCV Core-binding protein, is involved in the ubiquitin-independent degradation of the Core and HCV propagation [33,35,36]. However, little is known whether or not the ubiquitin modification of the Core might be involved in HCV egress like other enveloped viruses.

Finally, the identification of the site of viral particle assembly and budding is an intriguing issue. In case of HCV, at present, it is very difficult to visualize the HCV budding site in the infected cells by an electron microscopy. However, recent studies suggested that lipid droplets are an important cytoplasmic organelle for HCV production [4]. In this regard, Shavinskaya *et al.* demonstrated that

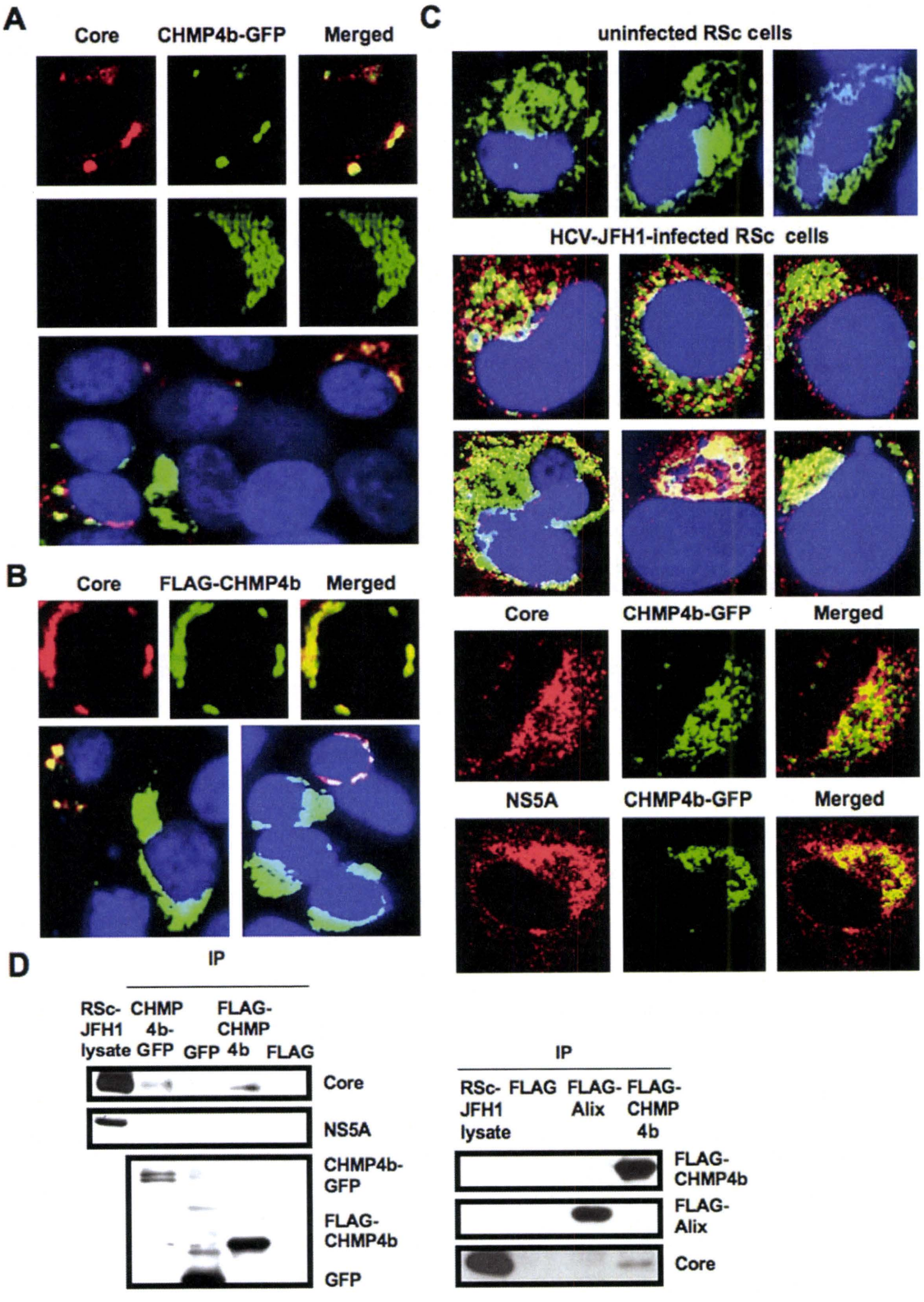

Figure 4. HCV Core interacts with CHMP4b. (A–C) HCV Core colocalizes with CHMP4b. 293FT cells cotransfected with 100 ng of pcDNA3/core (JFH1) and either 100 ng of pCHMP4b-GFP [39] (A) or pFLAG-CHMP4b [39] (B) were examined by confocal laser scanning microscopy. Cells were stained with anti-HCV Core and anti-FLAG polyclonal antibody and were then visualized with FITC (FLAG-CHMP4b) or Cy3 (Core). Images were visualized using confocal laser scanning microscopy. The right panels exhibit the two-color overlay images (Merged). Colocalization is shown in yellow. (C) The Core or NS5A partially colocalizes with CHMP4b in HCV-JFH1-infected RSc cells. RSc cells transfected with 100 ng of pCHMP4b-GFP were infected with HCV-JFH1. Cells were fixed 60 hrs post-infection and were then examined by confocal laser scanning microscopy as shown in panel (A). (D) HCV Core binds to CHMP4b. 293FT cells transfected with 4 μg of pCHMP4b-GFP, pEGFP C3 (Clontech), pcDNA3-FLAG, pcDNA3-FLAG-Alix or pFLAG-CHMP4b and RSc cells 5 days after inoculation of HCV-JFH1 at an MOI of 4 were lysed. The mixtures of these lysates were immunoprecipitated with either anti-FLAG or Living Colors A.v. monoclonal antibody (anti-GFP antibody), followed by immunoblot analysis using anti-HCV Core, anti-HCV NS5A, anti-FLAG, and/or Living Colors A.v. monoclonal antibody.
doi:10.1371/journal.pone.0014517.g004

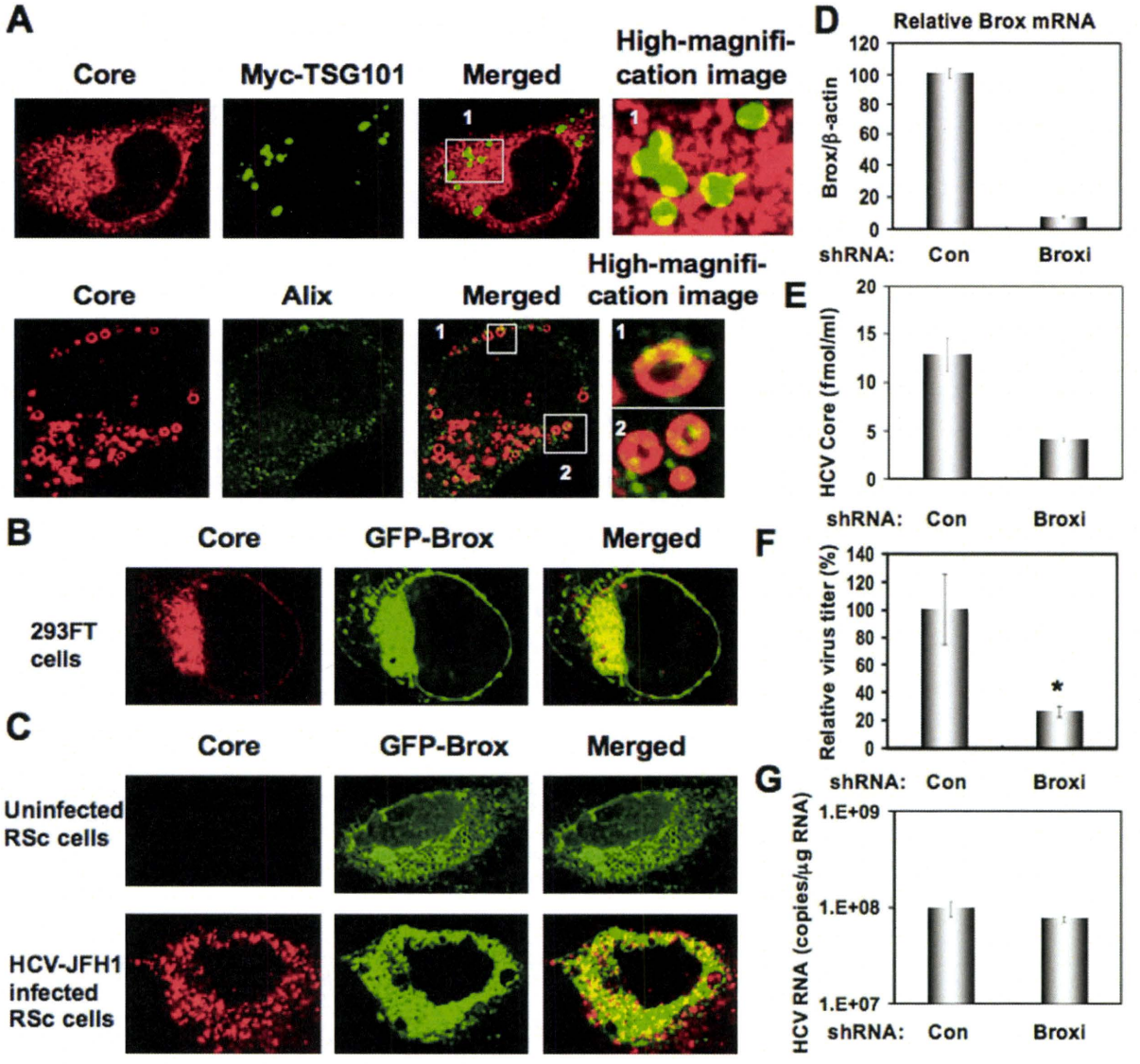

Figure 5. Brox is required for HCV life cycle. (A) Subcellular localization of Myc-tagged TSG101 in HCV-JFH1-infected RSc cells. RSc cells transfected with 100 ng of pBj-Myc-TSG101 [40] were infected with HCV-JFH1. Cells were fixed 60 hrs post-infection and were then examined by confocal laser scanning microscopy as shown in Fig. 3. High magnification image of area 1 is shown. Subcellular localization of endogenous Alix in HCV-JFH1-infected RSc cells 60 hrs post-infection. Cells were stained with anti-Alix and anti-HCV Core antibodies and were examined by confocal laser scanning microscopy. High magnification images of area 1 and area 2 are shown. (B) HCV Core partially colocalizes with Brox. 293FT cells cotransfected with 100 ng of pcDNA3/core (JFH1) and 100 ng of pmGFP-Brox^{WT} [27] were examined by confocal laser scanning microscopy. (C) The HCV Core partially colocalizes with Brox in HCV-JFH1-infected RSc cells. RSc cells transfected with 100 ng of pmGFP-Brox^{WT} were infected with HCV-JFH1. Cells were fixed 60 hrs post-infection and were then examined by confocal laser scanning microscopy. (D) Inhibition of Brox mRNA expression by the shRNA-producing lentiviral vector. Real-time LightCycler RT-PCR for Brox was performed as well as for β-actin mRNA in triplicate. Each mRNA level was calculated relative to the level in RSc cells transduced with a control lentiviral vector (Con) which was assigned as 100%. (E) The levels of HCV Core in the culture supernatants from the Brox knockdown RSc cells (Broxi) 72 hrs after inoculation of HCV-JFH1 were determined by ELISA. (F) The infectivity of HCV in the culture supernatants was determined by a focus-forming assay at 48 hrs post-infection. Experiments were done in triplicate and each virus titer was calculated relative to the level in RSc cells transduced with a control lentiviral vector (Con) which was assigned as 100%. Asterisks indicate significant differences compared to the control treatment. *$P<0.05$; **$P<0.01$. (G) The levels of intracellular genome-length HCV-JFH1 RNA in the cells used in (E) were monitored by real-time LightCycler RT-PCR.
doi:10.1371/journal.pone.0014517.g005

the lipid droplet-binding domain of the Core is a major determinant for efficient virus assembly [6]. The HCV Core induces lipid droplet redistribution in a microtubule- and dynein-dependent manner, since disrupting the microtubule network reduced the HCV titer, implicating transport networks in virus assembly and release [2]. Furthermore, Sandrin *et al.* reported that HCV envelope proteins localized to ESCRT-associated multivesicular body (MVB) [37]. Quite recently, Corless *et al.* have demonstrated that Vps4B and the ESCRT-III complex are required for HCV production [38]. Consistent with our findings, their dominant-negative forms of Vps4B and CHMP4B clearly suppressed HCV production. However, their dominant-negative forms of TSG101 and Alix failed to suppress the HCV production and they suggested that both TSG101 and Alix are unrelated to the HCV production. In contrast, we have demonstrated both TSG101 and Alix are also required for the infectious HCV

production by using shRNAs and siRNAs (Fig. 1). We may partly explain such discrepancy due to the difference of the methodology in our study utilized shRNAs and siRNAs instead of dominant-negative forms of TSG101 and Alix. Importantly, they demonstrated that the dominant-negative forms of Vps4B and CHMP4b did not affect the HCV RNA replication and the accumulation of intracellular infectious particles, suggesting that Vps4B and CHMP4b are unrelated to HCV RNA replication. Indeed, we have demonstrated that the ESCRT system is not required for the assembly of intracellular infectious HCV particles (Fig. 2E). Notably, we have demonstrated for the first time that HCV Core associated with CHMP4b (Fig. 4). Accordingly, we have also demonstrated that Brox, a CHMP4b binding protein, is required for HCV production (Fig. 5D–G). Taking together the past and present findings, we propose that the ESCRT system is involved in infectious HCV production after the HCV assembly that occurs on lipid droplets.

Acknowledgments

We thank D. Trono, R. Iggo, R. Agami, A. Takamizawa, and K. Shimotohno for pCMVΔR8.91, pMDG2, pSUPER, pRDI292, and anti-NS5A antibody, respectively. We also thank K. Abe for construction of pJRN/3-5B and T. Nakamura for his technical assistance.

Author Contributions

Conceived and designed the experiments: YA NK. Performed the experiments: YA MK. Analyzed the data: YA. Contributed reagents/materials/analysis tools: MM MI HD TW. Wrote the paper: YA NK.

References

1. Kato N, Hijikata M, Ootsuyama Y, Nakagawa M, Ohkoshi S, et al. (1990) Molecular cloning of the human hepatitis C virus genome from Japanese patients with non-A, non-B hepatitis. Proc Natl Acad Sci USA 87: 9524–9528.
2. Boulant S, Douglas MW, Moody L, Budkowska A, Targett-Adams P, et al. (2008) Hepatitis C virus core protein induces lipid droplet redistribution in a microtubule- and dynein-dependent manner. Traffic 9: 1268–1282.
3. Masaki T, Suzuki R, Murakami K, Aizaki H, Ishii K, et al. (2008) Interaction of hepatitis C virus nonstructural protein 5A with core protein is critical for the production of infectious virus particles. J Virol 82: 7964–7976.
4. Miyanari Y, Atsuzawa K, Usuda N, Watashi K, Hishiki T, et al. (2007) The lipid droplet is an important organelle for hepatitis C virus production. Nat Cell Biol 9: 1089–1097.
5. Shi ST, Polyak SJ, Tu H, Taylor DR, Gretch DR, et al. (2002) Hepatitis C virus NS5A colocalizes with the core protein on lipid droplets and interacts with apolipoproteins. Virology 292: 198–210.
6. Shavinskaya A, Boulant S, Penin F, McLauchlan J, Bartenschlager R (2007) The lipid droplet binding domain of hepatitis C virus core protein is a major determinant for efficient virus assembly. J Biol Chem 282: 37158–37169.
7. Murray CL, Jones CT, Tassello J, Rice CM (2007) Alanine scanning of the hepatitis C virus core protein reveals numerous residues essential for production of infectious virus. J Virol 81: 10220–10231.
8. Appel N, Zayas M, Miller S, Krijnse-Locker J, Schaller T, et al. (2008) Essential role of domain III of nonstructural protein 5A for hepatitis C virus infectious particle assembly. PLOS Pathog 4: e1000035.
9. Tellinghuisen TL, Foss KL, Treadaway J (2008) Regulation of hepatitis C virion production via phosphorylation of the NS5A protein. PLoS Pathog 4: e1000032.
10. Bieniasz PD (2006) Late budding domains and host proteins in enveloped virus release. Virology 344: 55–63.
11. Chen BJ, Lamb RA (2008) Mechanisms for enveloped virus budding: Can some viruses do without an ESCRT? Virology 372: 221–232.
12. Garrus JE, von Schwedler UK, Pornillos OW, Morham SG, Zavitz KH, et al. (2001) Tsg101 and vacuolar protein sorting pathway are essential for HIV-1 budding. Cell 107: 55–65.
13. Wakita T, Pietschmann T, Kato T, Date T, Miyamoto M, et al. (2005) Production of infectious hepatitis C virus in tissue culture from a cloned viral genome. Nat Med 11: 791–796.
14. Ariumi Y, Kuroki M, Abe K, Dansako H, Ikeda M, et al. (2007) DDX3 DEAD-box RNA helicase is required for hepatitis C virus RNA replication. J Virol 81: 13922–13926.
15. Ariumi Y, Kuroki M, Dansako H, Abe K, Ikeda M, et al. (2008) The DNA damage sensors, ataxia-telangiectasia mutated kinase and checkpoint kinase 2 are required for hepatitis C virus RNA replication. J Virol 82: 9639–9646.
16. Kuroki M, Ariumi Y, Ikeda M, Dansako H, Wakita T, et al. (2009) Arsenic trioxide inhibits hepatitis C virus RNA replication through modulation of the glutathione redox system and oxidative stress. J Virol 83: 2338–2348.
17. Ikeda M, Abe K, Dansako H, Nakamura T, Naka K, et al. (2005) Efficient replication of a full-length hepatitis C virus genome, strain O, in cell culture, and development of a luciferase reporter system. Biochem Biophys Res Commun 329: 1350–1359.
18. Ikeda M, Abe K, Yamada M, Dansako H, Naka K, et al. (2006) Different anti-HCV profiles of statins and their potential combination therapy with interferon. Hepatology 44: 117–125.
19. Ariumi Y, Kaida A, Hatanaka M, Shimotohno K (2001) Functional cross-talk of HIV-1 Tat with p53 through its C-terminal domain. Biochem Biophys Res Commun 287: 556–561.
20. Abe K, Ikeda M, Ariumi Y, Dansako H, Wakita T, et al. (2009) HCV genotype 1b chimeric replicon with NS5B of JFH-1 exhibited resistance to cyclosporine A. Arch Virol 154: 1671–1677.
21. Ariumi Y, Ego T, Kaida A, Matsumoto M, Pandolfi PP, et al. (2003) Distinct nuclear body components, PML and SMRT, regulate the trans-acting function of HTLV-1 Tax oncoprotein. Oncogene 22: 1611–1619.
22. Brummelkamp TR, Bernard R, Agami R (2002) A system for stable expression of short interfering RNAs in mammalian cells. Science 296: 550–553.
23. Bridge AJ, Pebernard S, Ducraux A, Nicoulaz AL, Iggo R (2003) Induction of an interferon response by RNAi vectors in mammalian cells. Nat Genet 34: 263–264.
24. Ariumi Y, Priscilla T, Masutani M, Trono D (2005) DNA damage sensors ATM, ATR, DNA-PKcs, and PARP-1 are dispensable for human immunodeficiency virus type 1 integration. J Virol 79: 2973–2978.
25. Naldini L, Blömer U, Gallay P, Ory D, Mulligan R, et al. (1996) In vivo gene delivery and stable transduction of non-dividing cells by a lentiviral vector. Science 272: 263–267.
26. Zufferey R, Nagy D, Mandel RJ, Naldini L, Trono D (1997) Multiply attenuated lentiviral vector achieves efficient gene delivery in vivo. Nat Biotechnol 15: 871–875.
27. Ichioka F, Kobayashi R, Katoh K, Shibata H, Maki M (2008) Brox, a novel farnesylated Bro1 domain-containing protein that associates with charged multivesicular body protein 4 (CHMP4). FEBS J 275: 682–692.
28. Chiou CT, Hu CCA, Chen PH, Liao CL, Lin YL, et al. (2003) Association of Japanese encephalitis virus NS3 protein with microtubules and tumor susceptibility gene 101 (TSG101) protein. J Gen Virol 84: 2795–2805.
29. Yi M, Ma Y, Yates J, Lemon SM (2007) Compensatory mutations in E1, p7, NS2, and NS3 enhance yields of cell culture-infectious intergenotypic chimeric hepatitis C virus. J Virol 81: 629–638.
30. Ma Y, Yates J, Liang Y, Lemon SM, Yi M (2008) NS3 helicase domains involved in infectious intracellular hepatitis C virus particle assembly. J Virol 82: 7624–7639.
31. Blanchard E, Hourioux C, Brand D, Ait-Goughoulte M, Moreau A, et al. (2003) Hepatitis C virus-like particle budding: Role of the core protein and importance of its Asp^{111}. J Virol 77: 10131–10138.
32. Klein KC, Dellos SR, Lingappa JR (2005) Identification of residues in hepatitis C virus core protein that are critical for capsid assembly in a cell-free system. J Virol 79: 6814–6826.
33. Moriishi K, Okabayashi T, Nakai K, Moriya K, Koike K, et al. (2003) Proteasome activator 28γ-dependent nuclear retention and degradation of hepatitis C virus core protein. J Virol 77: 10237–10249.
34. Shirakawa M, Murakami K, Ichimura T, Suzuki R, Shimoji T, et al. (2007) E6AP ubiquitin ligase mediates ubiquitylation and degradation of hepatitis C virus core protein. J Virol 81: 1174–1185.
35. Suzuki R, Moriishi K, Fukuda K, Shirakura M, Ishii K, et al. (2009) Proteasomal turnover of hepatitis C virus core protein is regulated by two distinct mechanisms: a ubiquitin-dependent mechanism and a ubiquitin-independent but PA28γ-dependent mechanism. J Virol 83: 2389–2392.
36. Moriishi K, Shoji I, Mori R, Suzuki R, Suzuki T, et al. (2010) Involvement of PA28gamma in the propagation of hepatitis C virus. Hepatology 52: 411–420.
37. Sandrin V, Boulanger P, Penin F, Granier C, Cosset FL, et al. (2005) Assembly of functional hepatitis C virus glycoproteins on infectious pseudoparticles occurs intracellularly and requires concomitant incorporation of E1 and E2 glycoproteins. J Gen Virol 86: 3189–3199.
38. Corless L, Crump CM, Griffin SD, Harris M (2010) Vps4 and ESCRT-III complex are required for the release of infectious hepatitis C virus particles. J Gen Virol 91: 362–372.
39. Katoh K, Shibata H, Suzuki H, Nara A, Ishidoh K, et al. (2003) The ALG-2-interacting protein Alix associates with CHMP4b, a human homologue of yeast Snf7 that is involved in multivesicular body sorting. J Biol Chem 278: 39104–39113.
40. Katoh K, Suzuki H, Terasawa Y, Mizuno T, Yasuda J, et al. (2005) The penta-EF-hand protein ALG-2 interacts directly with the ESCRT-I component TSG101, and Ca^{2+}-dependently co-localizes to aberrant endosomes with dominant-negative AAA ATPase SKD1/Vps4B. Biochem J 391: 677–685.